Renormalized Brueckner-Hartree-Fock calculations of ^{4}He and ^{16}O with center-of-mass corrections*

Richard L. Becker, K. T. R. Davies, and M. R. Patterson
Oak Ridge National Laboratory, Oak Ridge, Tennessee 37830

(Received 24 September 1973)

It is emphasized that the propagator-renormalized Brueckner-Hartree-Fock self-consistent field theory (RBHF) is an improvement over the unrenormalized Brueckner approximation plus rearrangement energy corrections for two main reasons: (i) through the renormalization of the off-diagonal matrix elements of the single-particle potential in a fixed basis the shape and size of the field are modified, leading to increased nuclear radii and improved density distributions which affect the expectation values of all observables; (ii) through the solution of coupled equations for the "true" occupation probabilities, occupancy-rearrangement effects are calculated self-consistently rather than merely to lowest order. For an accurate test of the RBHF approximation in light nuclei, center-of-mass (c.m.) corrections to the calculated properties are quite important. Two ways of making the c.m. corrections, discussed earlier, are applied and compared in calculations with the Reid soft-core and Hamada-Johnston interactions for ^{4}He and ^{16}O. The RBHF equations are solved by matrix diagonalization in the harmonic-oscillator basis. The well depth of the oscillator reference potential for virtual "particle" states is determined by requiring self-consistency, for the low-lying "particle" states, with an average off-energy-shell RBHF self-energy. The binding energies are in good agreement with experiment, as is the radius of ^{4}He, while the radius of ^{16}O is about 8% too small. A careful comparison of separation energies with experiment is made; c.m. corrections, the effect of spuriosity (presence of excited c.m. components) in the $0s_{1/2}$ hole state in ^{15}O or ^{15}N, and second- and third-order rearrangement energies calculated earlier, are included. Details of density distributions and electron elastic scattering form factors are given. The possible existence of a dip in the proton density at the center of the α particle is discussed. The need for higher dimensionality in the calculation of form factors and properties of unbound single-particle states is established.

[NUCLEAR STRUCTURE Renormalized Brueckner-Hartree-Fock method; c.m., rearrangement corrections. ^{4}He, ^{16}O; calculated binding, SP E's, separation E's, true occupation probabilities, ρ, e-scattering form factor.]

I. INTRODUCTION

The renormalized Brueckner-Hartree-Fock (RBHF) approximation for finite nuclei[1-4] is closely related to the simplest truncation[5,6] of Brandow's propagator-renormalized form[7] of the Brueckner-Goldstone series[8] for the binding energy. It has several features which may allow it to play for nuclear physics a role similar to that of the Hartree-Fock (HF) approximation in atomic and molecular physics. The great strength of nuclear forces renders HF theory inapplicable. The use of Brueckner's reaction matrix[8] as an effective interaction restores the possibility of an independent-particle description, but the single-particle (SP) energies and wave functions of the ordinary Brueckner-Hartree-Fock (BHF) approximation can differ greatly from those describing the removal or addition of a nucleon.[9] It is highly desirable, for economy in the calculation of the matrix elements of SP operators and of properties relating nucleus A to nuclei $A \pm 1$,[4,9,6] to reduce these differences by generalizing the self-consistent field. The RBHF approximation involves a modification of the field which takes into account the depletions of the normally occupied SP states resulting from two-nucleon correlations.

It has been shown both numerically[4,10] and analytically[10] that in the RBHF approximation the analog of "Koopmans's theorem" for the HF approximation[11] holds; namely, there is a near equality between the SP energies and separation energies. Both are theoretical quantities; the relation to experimental "centroids" is discussed below. The theoretical separation energies of the RBHF theory are defined as follows[2,4,10]: we assume that the RBHF binding energies $\mathcal{E}$ of the nuclei A and $(A \pm 1; v)$ have been calculated. Here v labels the SP "valence" hole or "particle" state in nucleus $A-1$ or $A+1$, respectively. (We put the word "particle" in quotation marks when it is used in the sense opposite to "hole".) The RBHF

"addition" energy associated with a valence "particle" state v_p is defined by

$$E(v_p) \equiv \mathcal{E}(A+1; v_p) - \mathcal{E}(A). \quad \text{(I.1)}$$

Similarly, for a valence hole v_h the negative of the "removal" energy is defined as

$$E(v_h) \equiv \mathcal{E}(A) - \mathcal{E}(A-1; v_h). \quad \text{(I.2)}$$

The analog of Koopmans's theorem is that, aside from center-of-mass (c.m.) corrections,

$$E(v) \approx e_v, \quad \text{(I.3)}$$

where e_v is the RBHF SP energy of the valence state. The "orbital rearrangement energy," associated with changes in the SP wave functions induced by the valence nucleon, is neglected in Koopmans's theorem and its analog. It is expected to be small when A is a doubly-closed-shell nucleus.[10]

The main difference between the RBHF and BHF approximations is that the RBHF SP potential U_{RBHF} includes along with the BHF contributions [Figs. 1(a) and 1(d)], which are factorizable by generalized time-ordering (g.t.o.),[12-15] also the contributions of Figs. 1(b) and 1(e), which are also g.t.o. factorizable.[12,16,7] By "factorizable" one means that in a ground-state diagram the insertion can be placed on the energy shell relative to the skeleton in which it is inserted and, hence, can be computed independently of the skeleton. In the Goldstone diagrams[8] of the present paper we follow the convention[15] in which a jagged line represents an on-energy-shell antisymmetrized reaction matrix element t_A and a wavy line is used for off-energy-shell matrix elements. Notice that Fig. 1 includes contributions only to hole-hole and hole-particle matrix elements of U. Similar insertions in "particle" lines, which when present in ground-state (closed) diagrams (e.g., Fig. 2) are not factorizable by g.t.o., are discussed separately in Sec. II.

In infinite nuclear matter the conservation of momentum in each interaction makes the particle-hole matrix elements, Figs. 1(d) and 1(e), vanish; and it makes $h = h'$ and $h_1 = h_1'$ in Figs. 1(a) and 1(b). Figure 1(b) was discussed first by Thouless[12] (see also Ref. 13) for nuclear matter. He pointed out its factorizability and estimated its value as about -14% of the BHF potential, which is rather close to the results of several modern calculations. Brueckner, Gammel, and Kubis[16] soon provided a detailed calculation giving for Fig. 1(b) about -8.4% of the BHF potential. Köhler obtained between -9 and -17.5%[17] (see also Ref. 18) and Brandow[19] and Wong[20] estimated it as -20% of the BHF potential. The first discussions of rearrangement effects in finite nuclei were given[21] in the context of the local density-dependent Hartree-Fock (DDHF) approach.[22] The first "global" calculations of Fig. 1(b) for finite nuclei (i.e., calculations

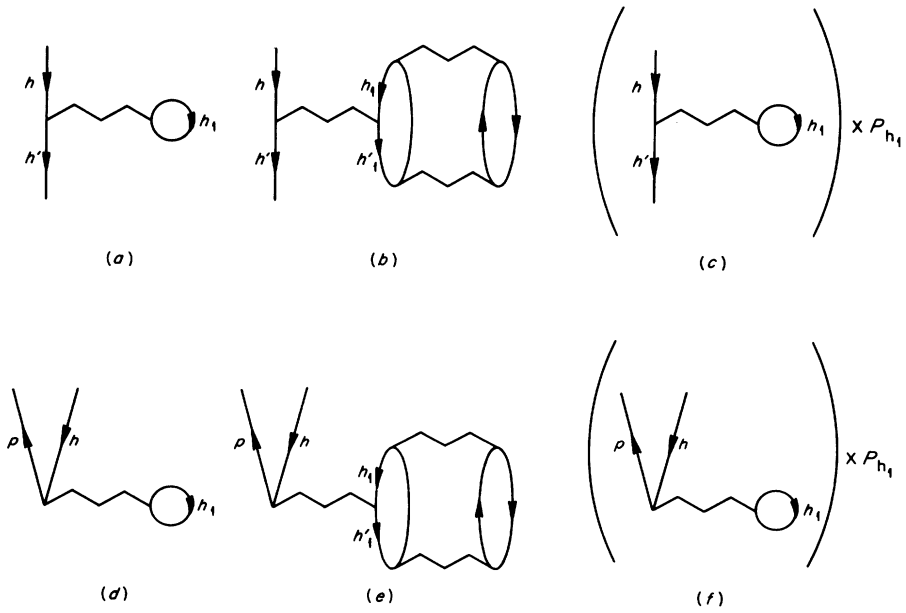

FIG. 1. Self-energy insertions contained in the RBHF-SP potential U. (a) Ordinary BHF insertion in a hole line. (b) Third-order saturation potential for a hole line. (c) RBHF insertion in a hole line. Figures 1(c), (d), and (e) are particle-hole creation diagrams resulting from a BHF insertion (d), a saturation potential insertion (e), and the full RBHF insertion (f).

employing Racah algebra and SP wave functions appropriate for a finite nucleus) were carried out by Wong,[20] followed by Köhler and McCarthy.[23] Wong obtained for it about −25% of the BHF potential for light nuclei. Whereas most previous work had emphasized the contribution of the short-range repulsion in the nuclear interaction, Wong found that the long-range attraction, mainly the tensor force, gave a comparable contribution.

Let us consider next the effect on the binding energy of the nucleus when Fig. 1(b) is included in the SP potential.[7,24,2] The presence of $X=-U$ in the residual interaction $H-(T+U)$ leads to diagrams for the binding energy containing insertions of X, e.g., that of Fig. 2(a). The part of U corresponding to Fig. 1(b), when substituted into Fig. 2(a) gives minus twice the contribution of the g.t.o. diagram for the binding energy shown in Fig. 2(b). In this diagram there are four energy denominators, each involving the SP energies of only two holes and two "particles." In contrast to this the Goldstone expansion (without g.t.o.) for the binding energy contains the diagrams of Figs. 2(c) and 2(d), in each of which two of the energy denominators involve the SP energies of four holes and four "particles." Summation of Figs. 2(c) and 2(d), which is equivalent to *one half* the sum of Fig. 2(c) over all four possible orderings of the interactions, leads to the factorized energy denominators of Fig. 2(b).[12a,16] When the bare interactions in Figs. 2(c) and 2(d) are replaced by reaction matrices, the generalized-time ordering also places the starting energies of all four reaction matrices on the energy shell.[7] In the summation of Fig. 2(c) over four orderings of the interactions each

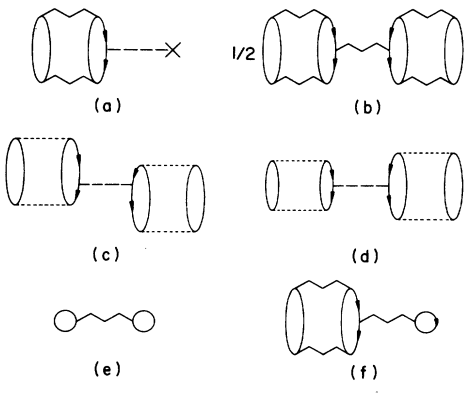

FIG. 2. Brueckner-Goldstone diagrams for the binding energy: (a) $X\equiv -U$ insertion in a hole line; (b) the g.t.o. contribution associated with the saturation potential, Fig. 1(b); (c) and (d) Goldstone diagrams contained in Fig. 2(b); (e) the ordinary BHF diagram; (f) contribution associated with the BHF potential, Fig. 1(a).

topologically distinct Brueckner-Goldstone diagram is counted twice. Consequently, Fig. 2(b) of the g.t.o. form of the Brueckner-Goldstone series, which has Figs. 2(c) and 2(d) as its lowest-order contributions, contains the factor $\frac{1}{2}$ shown in the diagram. We may now compare the binding energy in two different formulations,[2,24] both of which give ~1 MeV/nucleon more binding[12a,16] than the BHF approximation by including Fig. 2(b):
(i) If U does not contain Fig. 1(b), then Figs. 2(a) and 2(f) cancel each other, so the binding energy contains the BHF term [Fig. 2(e)] *plus* Fig. 2(b).
(ii) If U contains Fig. 1(b), then Fig. 2(a) includes minus twice Fig. 2(b), so the binding energy contains the BHF term, with more attractive matrix elements than before,[7,20,2,24] and *minus* Fig. 2(b).
In comparing (ii) with (i) the explicit difference, $(-2)\times$ Fig. 2(b), which is positive and small (~2 MeV/nucleon), is canceled[7,24] to first order in $\Delta e_h/e_h$ by the change in the value of the BHF term when the energies of the normally occupied states e_h are raised by Δe_h by the inclusion of Fig. 1(b) in U. Thus, (i) and (ii) give nearly equal binding energies. An intermediate formulation also has been suggested[12a]:
(iii) If U contains $\frac{1}{2}$ of Fig. 1(b), then Fig. 2(a) includes minus Fig. 2(b), so the binding energy contains only the BHF term, the value of which lies nearly midway between the BHF terms of (i) and (ii). This method of including the effect of Fig. 2(b) on the binding energy has been employed by Köhler and McCarthy.[23] The auxiliary SP energies of this method lie halfway between the BHF and [BHF + Fig. 1(b)] energies.

We believe that is was an important contribution of Brandow[19] to urge that the "saturation potential" [Figs. 1(b) and 1(e)] be included in the self-consistent field where it would "renormalize" the BHF term, rather than be calculated only perturbatively as a "rearrangement" correction to various quantities. In the perturbative approach only the hole-hole part [Fig. 1(b)] has been calculated. It contributes directly to separation energies. But as a part of the field U_{sat}, especially the particle-hole part [Fig. 1(e)] contributes to the SP wave functions and, hence, to all observables.[6] We shall see below that the inclusion of Fig. 1(e) results in a desirable increase in the radius. It is far simpler to include an extra contribution in the field than to calculate separately the corresponding corrections to a whole set of quantities such as the radius (or, more generally, the charge distribution), the form factors for stripping and pickup, electromagnetic moments, etc.[9,6]

Later, Brandow[7,25] obtained a more general formulation amounting to a thoroughgoing renormalization of the entire perturbation series. The

starting point for this development is Thouless's observation[12a] that the negative of Fig. 1(b) is equal to Fig. 1(a) times the second-order contribution to the depletion,[4] $d_h \equiv 1 - P_h$, of the normally occupied state h. Here P_h is the "true" fractional occupation probability in the perturbed ground-state wave function as opposed to the "model" occupation probability (the occupancy of the SP state h in the unperturbed ground state, the RBHF Slater determinant), which has the value unity. Brandow[7] discovered that occupation probability insertions are factorizable by g.t.o.[12-14] in general; i.e., all of them can be calculated independently of the "skeleton" in which they are inserted. Consequently, in the linked-cluster expansions each diagram containing no SP insertions can be generalized so as to include along with the original diagram a certain class of higher-order diagrams containing insertions associated with occupation probabilities. The contribution of the renormalized diagram is formally that of the original diagram multiplied by "line weighting" factors, which are P_h for each normally occupied state h and $1 - P_p$ for each normally unoccupied state p.[7]

Brandow's formulation also implies a specific definition of the SP potential, namely the sum of all self-energy insertions which are factorizable by g.t.o.[12-14] His scheme leads to a grouping of terms in "compact clusters,"[7,25] suggested by the work of Rajaraman and Bethe on the three-body cluster.[26] In the resulting propagator-renormalized series for the binding energy there are terms which compensate for "over counting" certain terms of the original series.[7,25] An example was given above in connection with Fig. 2. The overcounting corrections involve only the SP potential and the occupation probabilities and, consequently, do not require additional computation.

In the RBHF approximation[1-4] the SP potential for hole states is that of Fig. 1(c), which includes Figs. 1(a) and 1(b) and higher-order contributions to the occupation probabilities of the normally occupied SP states P_h. The occupation probabilities of the normally empty SP states P_p have been found to be small in doubly-closed-shell nuclei but to decrease slowly with excitation energy[27] (see Sec. IV). In the RBHF approximation the P_p's do not enter into the calculation of either the SP potential or the P_h's. (They do affect these quantities in higher approximations.[5]) This decoupling of the P_p's and P_h's in the RBHF approximation has the important consequence that in finite nuclei the P_h's satisfy a finite set of coupled algebraic equations.[2,4] The solution of these equations enables one to take into account occupation-rearrangement corrections self-consistently to all orders of perturbation theory. The resulting depletions differ[4] by 20–30% from those calculated to lowest order. It has been found especially convenient in RBHF calculations, where in order to achieve self-consistency one requires knowledge of the reaction matrix elements as a function of the "starting energy" E_s to calculate the P_h's in terms of $dt(E_s)/dE_s$.[7,28] The coupled equations take the form[28]

$$P_h = \left[1 - \sum_{\underline{h}'}^{\text{occ}} \left\langle \underline{h}\underline{h}' \left| \frac{dt(E_s)}{dE_s} \right| \underline{h}\underline{h}' \right\rangle_A \Big|_{E_s = e_{hh'}} P_{h'}\right]^{-1}, \tag{I.4}$$

with $e_{hh'} \equiv e_h + e_{h'}$, the sum of the SP energies. The matrix elements are antisymmetrized, as indicated by the subscript A, and the SP states are in the m scheme, $\underline{h} = (n_h l_h j_h m_h \tau_h) = (h m_h \tau_h)$. If one sets the $P_{h'}$'s equal to one and expands the right-hand side, one obtains

$$P_h \approx 1 + \sum_{\underline{h}'}^{\text{occ}} \left\langle \underline{h}\underline{h}' \left| \frac{dt_A(E_s)}{dE_s} \right| \underline{h}\underline{h}' \right\rangle \Big|_{E_s = e_{hh'}} . \tag{I.5}$$

With this approximation for P_h in Fig. 1(c), one obtains the contributions of Figs. 1(a) and 1(b). It is, however, relatively easy to solve Eq. (I.4) exactly, given the reaction matrix elements. This has been done in all the RBHF calculations cited in the paper. Typically, the calculated P_h's have values from 0.75 to 0.90 in the closed-shell nuclei.

In the lowest approximation[5] to the renormalized Brueckner-Brandow series the particle-particle matrix elements of the SP potential $\langle p' | U | p \rangle$ are zero. In defining the RBHF approximation,[1-4,6] however, an insertion in "particle" lines, which is a generalization of the HF particle-particle interaction, has been included. In the Brueckner-Goldstone series, with or without g.t.o., the BHF insertion in "particle" lines is off the energy shell. However, as has been discussed by Becker and Jones,[29] by rearranging the Goldstone linked-cluster expansion one can replace off-shell insertions by on-shell insertions plus correction terms which are represented by folded diagrams. Similarly, off-shell insertions can be replaced by average off-shell insertions plus correction terms. As in unrenormalized BHF calculations (e.g., Refs. 15 and 30), similarly in RBHF calculations in order to obtain sufficient binding it has proved essential to include an attractive potential for low-lying excited SP states. The potential employed in the present work is fully specified in Sec. II.

The initial renormalized calculations[1,2,4] were

done for ^{4}He, ^{12}C, ^{16}O, and ^{40}Ca with pure harmonic-oscillator wave functions. These may be referred to[15,31] as single-oscillator-configuration (SOC) calculations, or[30] as "Brueckner", as opposed to BHF, calculations. Relative to the unrenormalized Brueckner approximation, the renormalized Brueckner approximation gives[4] a significant raising of the SP energies in ^{4}He, ^{16}O, and ^{40}Ca, as expected from the calculation of Fig. 1(b) as a perturbation.[20,23] The renormalized Brueckner approximation also gives some additional binding energy ($\sim\frac{3}{4}$ MeV/nucleon in ^{16}O)[2,4] because, as explained above, the renormalized formulation contains a contribution which corresponds to including in the unrenormalized g.t.o. series a generalization of Fig. 2(b). This contribution in RBHF is expressible in terms of depletions of the normally occupied states as

$$\frac{1}{2}\sum_{\underline{hh}'} d_h d_{h'} \langle \underline{hh}' | t_A(e_{hh'}) | \underline{hh}' \rangle \ . \qquad \text{(I.6)}$$

Because the average depletion $\bar{d}$ increases with the nuclear density[19,18,20] (i.e., with decreasing nuclear radius), the contribution of Eq. (I.6) [or Fig. 2(b)], which is negative, tends to decrease the self-consistent radius relative to that given by ordinary BHF calculations which only include Fig. 2(e) and not Fig. 2(b). However, once Fig. 2(b) is included, we have seen that it makes essentially no difference in the binding energy whether the hole-hole matrix elements of the SP potential are renormalized or not. [Wong[20] had included the effect of U_{sat} on the BHF term by raising the starting energies, but omitted consideration of its contribution to Fig. 2(a), and so predicted a decrease of radius on shifting the SP energies by Fig. 1(b).]

Renormalization of the self-consistent field does give rise to a significant change in the predicted radius through the particle-hole matrix elements of the saturation potential Fig. 1(e).[2] (This effect does not occur in infinite nuclear matter where $\langle p|U|h\rangle \equiv 0$.) The existence of the shift of radius by renormalization can be inferred from SOC calculations of the second-order contribution to the binding energy[15,2] δE with and without renormalization. Curves of δE for ^{16}O as a function of the inverse oscillator range parameter α are shown in the upper part of Fig. 3, reproduced from Ref. 2. The oscillator shell-model radius is proportional to α^{-1} and δE is a measure of the deviation of the SOC wave functions from BHF (or RBHF) self-consistency. In the unrenormalized calculation (solid curve in Fig. 3) $|\delta E|$ attains its minimum at $\alpha = 0.47$ fm^{-1}, corresponding to a nuclear radius (uncorrected for c.m. motion or proton size) of 2.26 fm. The renormalized calculation (dashed curve) gives 2.41 fm, $6\frac{1}{2}\%$ larger. The latter lies very near the minimum of the first-order renormalized Brueckner energy, shown in the dashed curve of the lower part of Fig. 3, as expected from a stationary property of the RBHF approximation.[7,5] The increase of the self-consistent radius by the renormalization of the particle-hole matrix elements of U has been confirmed in true RBHF calculations[3] (see Secs. III and IV) in which the orbitals are allowed to deviate from pure oscillator ones. [See also Ref. 36 cited below in which Table III shows an increase of the radius of the neutron distribution in ^{40}Ca by 5% as a result of renormalization and Fig. 4 (Ref. 36) shows the proton and mass densities vs r for the unrenormalized and renormal-

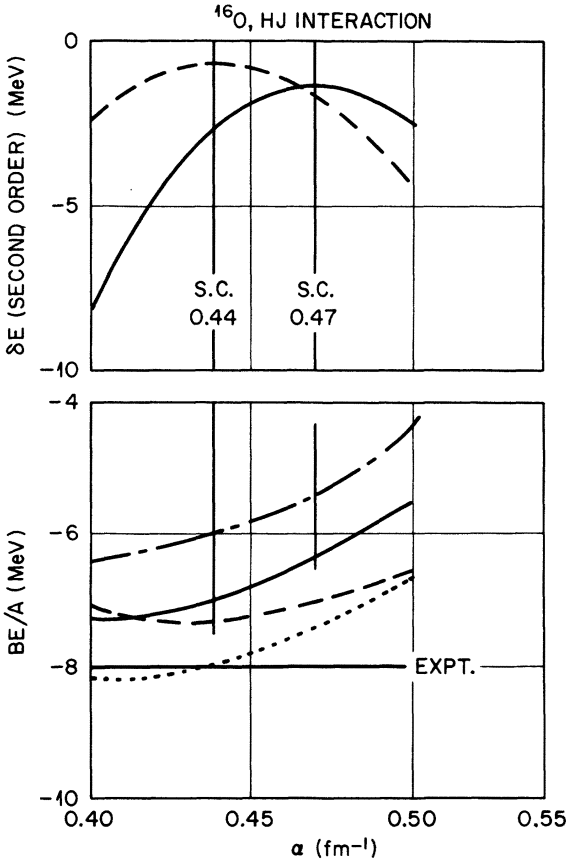

FIG. 3. SOC calculation of the second-order energy and the first-order energy per nucleon in ^{16}O as calculated in Ref. 2 from the Hamada-Johnston interaction (Ref. 56). The solid and dashed curves are for unrenormalized and renormalized calculations, respectively. The dotted curve is the unrenormalized BHF energy plus Fig. 2(b). The dashed-dotted curve is a renormalized calculation with $U_{RBHF} = \langle P_h \rangle U_{BHF}$, i.e., in which the shift of starting energies by renormalization is ignored.

ized calculations—the density at the origin is reduced by about $\frac{1}{8}$ by the renormalization.]

The calculation of Brueckner reaction matrices in a harmonic-oscillator basis has been shown to have several advantages.[15] Moreover, a growing body of calculations has demonstrated the utility of carrying out nuclear "matrix-HF" calculations by expanding the SP wave functions in a harmonic-oscillator basis, both for spherical[32,33] and deformed[34] states. Provision for energy dependence of the effective interaction in the matrix-HF method made possible (unrenormalized) matrix-BHF calculations for spherical nuclei.[30,35] The improvement of the radial SP wave functions over those in the SOC calculations leads to significant changes in the SP density distribution and to more accurate SP energies, particularly for SP states near the Fermi level.

The first renormalized calculations going beyond the SOC renormalized Brueckner approximation[1,2,4] were those of Ref. 3. The present paper includes a more detailed presentation of those RBHF calculations for ^{4}He and ^{16}O together with more recent work. An extensive RBHF calculation for the heavier spherical nuclei has recently been completed.[36] The initial BHF and RBHF results for deformed states also have been obtained.[37]

As discussed above, a chief merit of the RBHF approximation is that it provides a way out of the impasse, which occurs for the unrenormalized BHF theory, of requiring large rearrangement energies.[9] Another probably closely related way out of this difficulty is the density-dependent Hartree-Fock (DDHF) approach[22] in which the effective interaction is regarded as density-dependent. The DDHF SP potential then contains a Brueckner-Goldman "rearrangement potential"[22] in addition to the usual HF term. Impressive DDHF calculations have been performed recently for the spherical nuclei by Negele[38] with an effective interaction obtained by modifying the nuclear-matter reaction matrix elements calculated from the Reid soft-core interaction[39] by Siemens,[40] and applying them to finite nuclei in the local density approximation.[41] Deformed DDHF calculations for $12 \leq A \leq 40$ have been made with a linearized version of Negele's effective interaction by Zofka and Ripka.[42] Although the underlying justification for the DDHF ansatz[22] is still partially lacking, the effect of the rearrangement potential in DDHF is similar to that of the saturation potential in RBHF. The elucidation of the exact connection between the "global" RBHF and the "local" DDHF approaches should be quite instructive.

For the light nuclei c.m. corrections to the calculated ground-state properties are quite important. Recently, we have given a detailed discussion of possible treatments of c.m. effects in self-consistent field theories.[31]

The main purpose of the present paper is to compare the results of RBHF calculations for the lightest spherical closed-shell nuclei with experiment so as to provide a stringent test of the RBHF approximation. To establish accurately the results predicted by the RBHF theory, we have calculated c.m. corrections and have included second- and third-order rearrangement energy corrections obtained earlier.[6,27] In Sec. II the RBHF equations are reviewed. A detailed discussion is given of the prescription adopted for the excited state spectrum. Two ways of making c.m. corrections, referred to[31] as methods I and IIC, are presented. Sections III and IV contain the results for ^{4}He and ^{16}O, respectively. Of particular interest are new results on the convergence with dimensionality of the electron scattering form factor of ^{4}He, and the comparison of separation energies, including rearrangement energies, with experiment.

II. RBHF EQUATIONS WITH CENTER-OF-MASS CORRECTIONS

In any independent-particle model for finite nuclei the c.m. is not at rest. This is the case for all self-consistent field theories: HF, DDHF, BHF, RBHF, etc. For light nuclei c.m. corrections are of sufficient magnitude to be important in comparing theoretical and experimental quantities such as ground-state binding energies, separation energies, and radii. The basic equations of the RBHF approximation, including c.m. effects, were described in Ref. 31. Among several possibilities two "methods," denoted by I and IIC, were favored.

Method I

In method I the self-consistent field and determinantal wave function are calculated without including any correction for c.m. motion. However, the binding energy, separation energies, and radii are corrected for c.m. motion.

The RBHF SP potential[4] has matrix elements involving hole states given in the RBHF basis by (for the symmetrization see Refs. 15 and 43):

$$\langle \mathrm{h}' | U | \mathrm{h} \rangle = \sum_{\underline{\mathrm{h}}''} \langle \underline{\mathrm{h}}' \underline{\mathrm{h}}'' | \tfrac{1}{2}[t_A(e_{\mathrm{h}'\mathrm{h}''}) + t_A(e_{\mathrm{hh}''})] | \underline{\mathrm{h}}\underline{\mathrm{h}}'' \rangle P_{\mathrm{h}''} , \tag{II.1a}$$

$$\langle \mathrm{p} | U | \mathrm{h} \rangle = \langle \mathrm{h} | U | \mathrm{p} \rangle = \sum_{\underline{\mathrm{h}}'} \langle \underline{\mathrm{p}}\underline{\mathrm{h}}' | t_A(e_{\mathrm{hh}'}) | \underline{\mathrm{h}}\underline{\mathrm{h}}' \rangle P_{\mathrm{h}'} , \tag{II.1b}$$

where normally occupied states are labeled h, h′, etc., whereas states labeled p or p′ are normally empty. We recall that underlined labels of SP states refer to the m scheme; e.g., $\underline{h}=(hm_h\tau_h)$ with $h=(n_h l_h j_h)$.

The "particle-particle" matrix elements of U, which are critical for the determination of the spectrum and wave functions of virtual "particle" states, require some discussion. In the Brueckner-Brandow series[7,24,25,44] only those self-energy insertions which are exactly factorizable by g.t.o. are included in U. The BHF ("bubble") insertion in "particle" lines does not factorize by g.t.o., so Brandow's $\langle p'|U|p\rangle$ does not contain a contribution of first order in the reaction matrix. On the other hand, in the earlier propagator-unrenormalized work on nuclear matter[45,14] and finite nuclei[15] an average-off-shell BHF contribution was included, the average being taken with respect to the lowest-order (third-order) diagram (for the ground-state energy) in which it appears, Fig. 4. In connection with the more recent and satisfactory cluster ordering of the Brueckner-Goldstone series (the "hole-line" expansion[26]), Bethe has suggested defining the potential energy of "particle" states from the propagator-unrenormalized full three-body cluster, rather than from its third-order terms, thus generalizing the concept of an average-off-shell potential. An alternative, propagator-renormalized expansion,[46,47] involving an extension of g.t.o.,[29] contains an on-shell RBHF potential for "particles" together with an RBHF contribution to the line-weighting factors for "particles." This expansion also can be cluster ordered, and there is no conflict between including an RBHF potential for "particles" and evaluating the full renormalized three-body cluster.[47] The various approaches to the "particle"-state potential have been reviewed in Ref. 6 and, more extensively, in Ref. 47.

In the calculations of the present paper the matrix elements $\langle p'|U|p\rangle$ involving *low-lying* virtual "particle" states, i.e., those involved in the matrix-HF diagonalization procedure, are defined by an RBHF self-energy.[1-4,6] In the RBHF basis

$$\langle p'|U|p\rangle=\sum_{\underline{h}}\langle \underline{p'h}|\tfrac{1}{2}[t_A(\bar{e}_{p'}+e_h)+t_A(\bar{e}_p+e_h)]|\underline{ph}\rangle P_h\,, \tag{II.1c}$$

where $\bar{e}_p$ (in the notation of Refs. 30, 35, and 36) is an energy which, for virtual states, differs from the SP energy e_p by an average excitation energy of the medium.[15]

Equations (II.1) were given in the RBHF basis. The form which they assume in the oscillator basis has been discussed in Refs. 30, 35, and 37. The dependence of the reaction matrices on the starting energy, $e_{hh'}=e_h+e_{h'}$ etc., is the greatest source of difficulty in carrying out BHF as compared with HF calculations. It complicates the transformation of U into the oscillator basis and also necessitates storing many more two-body matrix elements. The SP wave functions of the normally occupied (hole) states satisfy

$$[T+U(e_h)-e_h]\phi_h=0\,, \tag{II.2}$$

where T is the SP kinetic-energy operator. In the matrix-BHF work these equations are solved as matrix equations in the oscillator basis. For the virtual "particle" states

$$[T+U(\bar{e}_p)-e_p]\phi_p=0\,. \tag{II.3}$$

In our work

$$\bar{e}_p=e_p-\delta e_p\,, \tag{II.4}$$

where δe_p is the average excitation energy of the remainder of the nucleus when state p is virtually occupied.[8] The matrix elements in Eq. (II.1c) are said to be off the energy shell.

For the calculation of "addition" energies we also calculate the SP energies and wave functions of valence "particles" in nucleus $(A+1)$[2,4,6,10] which satisfy

$$[T+U(E_p)-E_p]\psi_p=0. \tag{II.5}$$

The matrix elements of U occurring here are on the energy shell and can be regarded as satisfying Eq. (II.1c) with $\bar{e}_p=E_p$.

We hasten to add that in the present calculations, as in the other matrix-BHF and RBHF calculations performed up till now,[30,3,35,28,36,37,48,49] the virtual excited-state spectrum is not calculated completely self-consistently. The energies e_p of the virtual RBHF basis states are not fed back into the reaction operator. Such a feedback would require recalculation of the reaction matrix elements in the oscillator basis. Instead, a reference excited-state spectrum of fixed form, but with an adjustable parameter, a well-depth C, is used.[15] The reference SP potential for

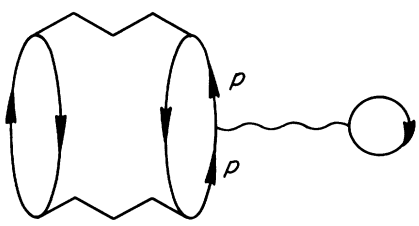

FIG. 4. Diagram for the binding energy containing an off-energy-shell BHF insertion in a "particle" line.

excited oscillator states is

$$U^R(r) = -C + \tfrac{1}{2}m\omega^2 r^2, \tag{II.6a}$$

resulting in the reference spectrum

$$e^R_{nlj} = e^{\rm osc}_{nl} - C. \tag{II.6b}$$

This has the advantage[15,50] that the energy denominators in the reaction matrices take the form

$$E_s - (e_{\rm p} + e_{\rm p'}) = E'_s - (e^{\rm osc}_{\rm p} + e^{\rm osc}_{\rm p'}), \tag{II.7a}$$

with the shifted starting energy

$$E'_s = E_s + 2C. \tag{II.7b}$$

The well depth C was determined so as to make the energies e_{nlj} of the SP states of the lowest two normally empty major shells self-consistent on the average: $\langle e\rangle = \langle e^R\rangle$. The self-consistency condition was that of Eqs. (II.1c), (II.3), and (II.4). For the average excitation energy [$\delta e_{\rm p}$ in Eq. (II.4)] an approximation recommended by Morris and Becker[51] and employed in Refs. 1–4, 30, 35, and 10 was used, namely

$$\delta e_{\rm p} = 2(e_{\rm p} - \langle e_{\rm h}\rangle), \tag{II.8a}$$

where $\langle e_{\rm h}\rangle$ is the weighted average of the energies of the normally occupied states. In this approximation

$$\bar{e}_{\rm p} = 2\langle e_{\rm h}\rangle - e_{\rm p}. \tag{II.8b}$$

Calculations by Morris[52,53] have shown that the use of Eq. (II.8a) yields results which differ only slightly from the exact evaluation of the Brueckner-Goldstone diagram of Fig. 4 for low-lying particle states p. The intermediate reaction matrix element in Fig. 4 is off the energy shell by an amount which varies with the other "particle" and the two holes present in the virtual excitation. In the renormalized theory the BHF insertion is multiplied by an occupation probability $P_{\rm h}$ for the hole. The choice of excited-state spectrum employed here and in earlier work[15,1-4,10] is somewhat analogous to that of Brueckner *et al.*[45] (see also Ref. 14) in the early nuclear-matter work, but differs in that the average-off-shell self-consistency is imposed only for low-lying states. As mentioned before, our reference spectrum differs strongly from the prescription, $\langle {\rm p'}|U|{\rm p}\rangle \approx 0$, of the "compact-cluster" expansion[7,25]; e.g., our $\langle {\rm p}|U|{\rm p}\rangle$ is negative for low-lying "particle" states and is increasingly more positive for higher-lying ones. The upper part of the spectrum is not self-consistent. However, the results of the calculations have been thought sensitive primarily to the lower part of the spectrum.[15] McCarthy[54] has introduced a downward shift $2B_0$ of only the low-lying part of the spectrum for *pairs* of virtual "particles." (The "particle" spectrum affects the reaction matrix only in pair states. If the entire "particle" spectrum is shifted downward by C, then the entire "particle"-pair spectrum is shifted by $2C$.) In Table IV of Ref. 36 one can see that a shift of $\bar{N}-8=18$ pair shells gave in ^{40}Ca an increase in binding of about half as much as the same shift of all "particle"-pair shells. An effective mass m^* for the virtual "particle" states of the oscillator basis has been introduced by Becker, Morris, and Patterson.[55] By varying both C and m^* one can vary the high-lying part of the spectrum while preserving Eq. (II.1c) for the low-lying part. Such a refinement has not yet been incorporated into the matrix-RBHF calculations.

It was noticed in our calculations[3] that the ϕ_n's and $e_{\rm h}$'s (of normally occupied states) were independent of whether the normally empty states were treated as virtual or valence ones. This fact is explained[35] as a consequence of the fixed reference spectrum. If the propagator in the reaction operator were defined in the RBHF basis, rather than by the fixed reference spectrum, the RBHF occupied-state wave functions and energies would vary with the prescription for $\bar{e}_{\rm p}$. A related effect, the dependence of the $e_{\rm h}$'s on the well depth C has been studied.[36,54] Also, the effect of shifting C on the radii, including the contributions of some diagrams of higher than first order, has been investigated.[49]

The binding energy with c.m. corrections is given in the RBHF basis by several alternative forms, e.g.,

$$\mathcal{E}^{\rm I} = \sum_{\underline{\rm h}} \langle h|T|h\rangle + \frac{1}{2}\sum_{\underline{\rm h}\underline{\rm h}'} \langle \underline{\rm h}\underline{\rm h}'|t_A(e_{\underline{\rm h}\underline{\rm h}'})|\underline{\rm h}\underline{\rm h}'\rangle P_{\rm h} P_{\rm h'}$$

$$+ \sum_{\underline{\rm h}} (1-P_{\rm h})\langle {\rm h}|U|{\rm h}\rangle - \langle \Psi^{\rm I}|\mathcal{J}_{\rm c.m.}|\Psi^{\rm I}\rangle \tag{II.9a}$$

$$= \sum_{\underline{\rm h}} (1-\tfrac{1}{2}P_{\rm h})\langle {\rm h}|U|{\rm h}\rangle + \langle \Psi^{\rm I}|\mathcal{J}_{\rm in}|\Psi^{\rm I}\rangle \tag{II.9b}$$

$$= \frac{1}{2}\sum_{\underline{\rm h}\underline{\rm h}'} (1-d_{\rm h}d_{\rm h'})\langle \underline{\rm h}\underline{\rm h}'|t_A(e_{\underline{\rm h}\underline{\rm h}'})|\underline{\rm h}\underline{\rm h}'\rangle + \langle \Psi^{\rm I}|\mathcal{J}_{\rm in}|\Psi^{\rm I}\rangle, \tag{II.9c}$$

as discussed in Ref. 31. The internal kinetic-energy operator $\mathcal{J} - \mathcal{J}_{\rm c.m.}$ is denoted by $\mathcal{J}_{\rm in}$. The occupation probabilities are calculated from Eq. (I.4). The analog of Koopmans's theorem [Eq. (I.3)] becomes modified by c.m. corrections to

$$E^{\rm I}(v_{\rm p}) \approx e^{\rm I}_{v_{\rm p}} - (A+1)^{-1}\left[\langle v_{\rm p}|T|v_{\rm p}\rangle - m^{-1}\sum_{\underline{\rm h}=1}^{A} |\langle \underline{v}_{\rm p}|\vec{\rm p}|\underline{\rm h}\rangle|^2 - \langle \Psi^{\rm I}(A)|\mathcal{J}_{\rm c.m.}|\Psi^{\rm I}(A)\rangle\right] \tag{II.10a}$$

and

$$E^{\mathrm{I}}(v_{\mathrm{h}}) \approx e^{\mathrm{I}}_{v_{\mathrm{h}}} - (A-1)^{-1}\left[\langle v_{\mathrm{h}}|T|v_{\mathrm{h}}\rangle - m^{-1}\sum_{\underline{\mathrm{h}}'=1}^{A}|\langle v_{\mathrm{h}}|\vec{\mathrm{p}}|\underline{\mathrm{h}}'\rangle|^2 - \langle\Psi^{\mathrm{I}}(A)|\mathcal{J}_{\mathrm{c.m.}}|\Psi^{\mathrm{I}}(A)\rangle\right] \quad \text{(II.10b)}$$

which are Eqs. (6.2) and (6.4) of Ref. 31.

Method IIC

In method II the RBHF equations are derived from the internal Hamiltonian, $\mathcal{K}_{\mathrm{in}} = \mathcal{K} - \mathcal{J}_{\mathrm{c.m.}}$, so that the SP wave functions and energies contain c.m. "corrections." In the version of method II referred to as IIC[31] the nuclear interaction is treated in renormalized fashion, but the two-body part of $\mathcal{J}_{\mathrm{c.m.}}$, which involves $\vec{\mathrm{p}}(1)\cdot\vec{\mathrm{p}}(2)$, is treated as in unrenormalized BHF. The reason for not renormalizing the contribution of $\vec{\mathrm{p}}(1)\cdot\vec{\mathrm{p}}(2)$ is that in RBHF the lack of a sum over the normally empty states with weighting factors P_{p}, while weighting the sums over normally occupied ones by P_{h}, could lead to serious errors. For the terms containing nucleon-nucleon interactions, on the other hand, the off-energy-shell propagation in excited states greatly weakens the terms containing states p, and the effect on the energy of terms involving P_{p} appears to be small in doubly-closed major shell nuclei.[27] However, the question of the magnitude of the leading corrections to the RBHF approximation[5] warrants considerable additional study.

In method IIC the effective SP potential is (k = h or p)

$$\langle k'|U^{\mathrm{IIC}}|k\rangle = \langle k'|U + U_{\mathrm{c.m.}}|k\rangle\,, \quad \text{(II.11a)}$$

where U is as defined by Eqs. (II.1) for method I, and

$$\langle k'|U_{\mathrm{c.m.}}|k\rangle = (Am)^{-1}\sum_{\underline{\mathrm{h}}''}\langle\underline{k}'|\vec{\mathrm{p}}|\underline{\mathrm{h}}''\rangle\cdot\langle\underline{\mathrm{h}}''|\vec{\mathrm{p}}|\underline{k}\rangle\,. \quad \text{(II.11b)}$$

For $k = k'$ Eqs. (II.11) are Eqs. (5.23) and (5.24) of Ref. 31. The SP wave functions and energies satisfy

$$[(1-A^{-1})T + U + U_{\mathrm{c.m.}} - e^{\mathrm{IIC}}_{k}]\phi^{\mathrm{IIC}}_{k} = 0\,. \quad \text{(II.12)}$$

The binding energy is given in the RBHF basis by

$$\mathcal{E}^{\mathrm{IIC}} = \sum_{\underline{\mathrm{h}}}(1-A^{-1})\langle\mathrm{h}|T|\mathrm{h}\rangle + \frac{1}{2}\sum_{\underline{\mathrm{h}}\underline{\mathrm{h}}'}[\langle\underline{\mathrm{h}}\underline{\mathrm{h}}'|t(e_{\mathrm{hh}'})|\underline{\mathrm{h}}\underline{\mathrm{h}}'\rangle P_{h}P_{h'} + (Am)^{-1}|\langle\underline{\mathrm{h}}|\vec{\mathrm{p}}|\underline{\mathrm{h}}'\rangle|^2] + \sum_{\underline{\mathrm{h}}}(1-P_{\mathrm{h}})\langle\mathrm{h}|U|\mathrm{h}\rangle \quad \text{(II.13a)}$$

$$= \sum_{\underline{\mathrm{h}}}(1-\tfrac{1}{2}P_{h})\langle\mathrm{h}|U|\mathrm{h}\rangle + \langle\Psi^{\mathrm{IIC}}|\mathcal{J}_{\mathrm{in}}|\Psi^{\mathrm{IIC}}\rangle\,. \quad \text{(II.13b)}$$

Notice that Eq. (II.13b) is formally the same as Eq. (II.9b), but that the SP wave functions, the starting energies in the reaction matrices appearing in U [Eqs. (II.1)], and the occupation probabilities are different from those of method

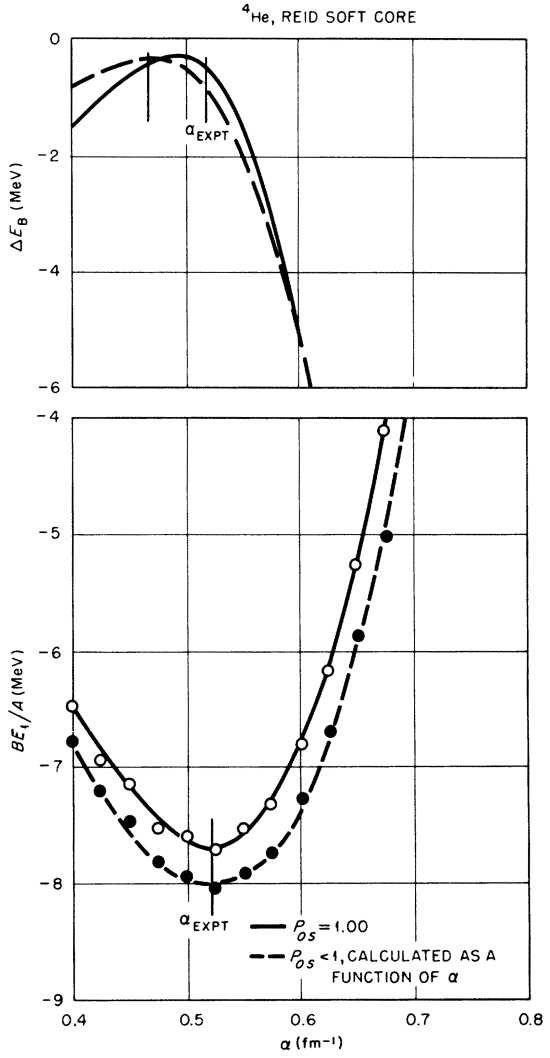

FIG. 5. Second-order contribution to the binding energy ΔE_B and first-order binding energy per nucleon BE_1/A for ^{4}He calculated in Ref. 2 in the unrenormalized (solid line) and renormalized (dashed line) SOC, Brueckner approximation. The Reid soft-core interaction (Ref. 39) was used. The unrenormalized BE_1/A does not include Fig. 2(b).

I, so that $\mathcal{G}^{I}$ and $\mathcal{G}^{IIC}$ will not be exactly the same.

The SP energies in method IIC differ from those of method I because e_k^I contains essentially a fraction $1/A$ of the kinetic energy of the center of mass, whereas this has been removed from e_k^{IIC}. As mentioned in Ref. 31, if we can ignore the starting energy and wave function differences between methods I and IIC, the SP energies are related by

$$e_k^{IIC} \approx e_k^I - A^{-1}\left(\langle k|T|k\rangle - m^{-1}\sum_{\underline{h}=1}^{A}|\langle \underline{k}|\vec{p}|\underline{h}\rangle|^2\right). \tag{II.14}$$

Then Eq. (II.10) can be rewritten as in Eq. (6.4) of Ref. 31:

$$E^I(v) = e_v^{IIC} + (A \pm 1)^{-1}[\langle \Psi^I(A)|\mathcal{G}_{c.m.}|\Psi^I(A)\rangle \pm (e_v^I - e_v^{IIC})]. \tag{II.15}$$

The separation energies in method IIC are given by

$$E^{IIC}(v) = e_v^{IIC} + (A \pm 1)^{-1}\left[\langle \Psi^{IIC}|\mathcal{G}_{c.m.}|\Psi^{IIC}\rangle \pm A^{-1}\left(\langle v|T|v\rangle - m^{-1}\sum_{\underline{h}=1}^{A}|\langle \underline{v}|\vec{p}|\underline{h}\rangle|^2\right)\right], \tag{II.16}$$

or, when (II.14) holds,

$$E^{IIC}(v) \approx e_v^I + (A \pm 1)^{-1}\left(\langle \Psi^{IIC}|\mathcal{G}_{c.m.}|\Psi^{IIC}\rangle - \langle v|T|v\rangle + m^{-1}\sum_{\underline{h}=1}^{A}|\langle \underline{v}|\vec{p}|\underline{h}\rangle|^2\right) \tag{II.17}$$

$$\approx E^I(v) + (A \pm 1)^{-1}(\langle \Psi^{IIC}|\mathcal{G}_{c.m.}|\Psi^{IIC}\rangle - \langle \Psi^I|\mathcal{G}_{c.m.}|\Psi^I\rangle). \tag{II.18}$$

III. CALCULATIONS FOR ^{4}He WITH THE REID SOFT-CORE AND HAMADA-JOHNSTON (HARD-CORE) INTERACTIONS

The lightest closed-shell nucleus, ^{4}He, provides a stringent test of any self-consistent field approximation because there are so few particles that the virtual excitation of even a single nucleon considerably alters the field felt by the others. Another way of expressing this is to remark that terms of order A^{-1}, where A is the nucleon number, are important for ^{4}He. We have included c.m. corrections, which are of order A^{-1}, but have not included several other refinements of this order.

Figure 5 (from Ref. 2) shows the BHF and RBHF binding energy per nucleon of ^{4}He calculated with SOC wave functions as a function of the inverse range parameter of the oscillator potential

$$\alpha = \left(\frac{M\omega}{2\hbar}\right)^{1/2} = 1/\sqrt{2}b. \tag{III.1}$$

The Reid soft-core interaction[39] was used. The renormalized calculation exhibits $\frac{1}{4}$ to $\frac{1}{2}$ MeV greater binding per nucleon than the BHF calculation, which does not include Fig. 2(b). The value of α which would yield the experimental value of the rms radius of ^{4}He (in the independent-particle-model approximation) is denoted by α_{expt}. The minima of both the BHF and RBHF curves are seen to occur at $\alpha = \alpha_{expt}$. The SOC wave functions do not exactly satisfy the RBHF self-consistency condition [Eq. (II.1b) for RBHF and Eq. (II.1b) without the factor $P_{\underline{h}'}$ for BHF]. This condition plays the role of the Brillouin condition of HF theory. As mentioned in Sec. I, a measure of the failure to satisfy the self-consistency condition is the second-order energy[15] denoted here by ΔE_B. It is seen in the upper part of Fig. 5 that ΔE_B is small in the neighborhood of $\alpha = 0.5$ fm^{-1} both for BHF and RBHF, indicating that SOC wave functions are nearly self-consistent for $\alpha \approx 0.5$ fm^{-1}. A slightly larger radius is indicated for the renormalized calculation.

In Table I we present results of the matrix-RBHF calculations of ^{4}He with methods I and IIC. For each method both the Reid soft-core[39] and Hamada-Johnston[56] (hard-core) interaction (HJ) have been used. In general we expand the RBHF wave function for a state $\psi_{\nu lj}$, where ν is a radial quantum number, in terms of oscillator wave functions ϕ_{nlj}. With the expansion coefficients denoted by $C_n^{\nu}(lj)$, we have

$$\psi_{\nu lj} = \sum_n C_n^{\nu}(lj)\phi_{nlj}. \tag{III.2}$$

In ^{4}He only the $0s_{1/2}$ RBHF state is occupied. The oscillator basis for the matrix-HF diagonalization contained s states with $n = 0$ through 3 (a "dimen-

sionality" D of 4). Table I lists the $0s_{1/2}$ neutron and proton SP and removal energies; the coefficients $C_n^0(0_{1/2})$ of the neutron and proton wave functions; the "true" occupation probability P_{0s}; the binding energy per nucleon; and the rms radii (corrected for the spread of the position of the center of mass[31]) of the mass distribution (assuming point nucleons) r_m, of the distribution of point neutrons r_n, and of charge (assuming a proton mean square radius of 0.64 fm^2) r_c.

By comparing the results of methods I and IIC, we see that the occupation probabilities change only slightly, but that for IIC the $0s_{1/2}$ neutron and proton energies are lowered by 4–5 MeV, and the rms charge radius decreases by about 7% to a value in much better agreement with experiment. These changes occur because in method IIC we have included c.m. corrections directly in the self-consistent part of the calculation. In both methods the binding energy has been corrected for c.m. motion; the small difference in the binding energies for the two methods is due to the differences in the self-consistency conditions. The $0s_{1/2}$ wave functions obtained in method IIC appear to be closer to the pure $0s_{1/2}$ oscillator wave functions (for $\alpha = 0.65$ fm^{-1}) than those obtained in method I; this corresponds to the smaller rms radius, which results from the reduction of the kinetic-energy part of the SP Hamiltonian in method IIC.

The calculations with the Reid interaction give greater binding and lower SP energies than those with the HJ interaction. Some of this increased binding is produced by the slightly larger "self-consistent" value of the oscillator well depth C for the Reid interaction; but the Reid matrix elements entering into the potential energy of the $0s_{1/2}$ state are also a little more attractive than those of the Hamada-Johnston interaction at the same value of E_s'. The generally greater attraction of the Reid interaction, associated with the soft core, has shown up in previous calculations.[4]

Table II gives results concerning the normally empty $0p_{3/2}$ and $0p_{1/2}$ shells. Just as for the nor-

TABLE I. RBHF calculations of the ground-state properties of ^{4}He for methods I and IIC. The dimensionality is 4; $\alpha = 0.65$ fm^{-1}; $C = 63.0$ MeV for the Reid (soft-core) interaction, and $C = 60.3$ for the Hamada-Johnston (HJ) interaction. Here and in all other tables of this paper energies are in MeV and radii in femtometers. The binding energy per nucleon ($\mathcal{E}/A$) and radii of the mass, neutron, and charge distributions (r_m, r_n, r_c) contain c.m. corrections. RBHF-SP energies are denoted by e, separation energies by E, and "true" occupation probabilities by P.

Method	I			IIC	
Interaction	Reid	HJ	Expt.	Reid	HJ
$-\mathcal{E}/A$	7.26	6.76	7.05	7.08	6.48
r_m	1.54	1.53		1.41	1.41
r_n	1.54	1.53		1.41	1.41
r_c	1.73	1.73	1.63 ± 0.04 [a]	1.62	1.63
			Neutrons		
$P_{0s_{1/2}}$	0.88	0.87		0.87	0.85
$-e_{0s_{1/2}}$	18.4	17.1		23.2	21.5
$-E_{0s_{1/2}}$	≈ 19.8 [b]		20.6 [c]	≈ 18.9 [b]	
$C_0^0(s_{1/2})$	0.9438	0.9455		0.9722	0.9707
$C_1^0(s_{1/2})$	−0.3059	−0.3039		−0.2235	−0.2307
$C_2^0(s_{1/2})$	0.1146	0.1089		0.0615	0.0606
$C_3^0(s_{1/2})$	−0.0495	−0.0423		−0.0332	−0.0292
			Protons		
$P_{0s_{1/2}}$	0.88	0.87		0.87	0.85
$-e_{0s_{1/2}}$	17.7	16.5		22.4	20.8
$-E_{0s_{1/2}}$	≈ 19.05 [b]		19.8 [c] 20.4 ± 0.3 [d]	≈ 18.1 [b]	
$C_0^0(s_{1/2})$	0.9434	0.9447		0.9715	0.9700
$C_1^0(s_{1/2})$	−0.3080	−0.3059		−0.2260	−0.2331
$C_2^0(s_{1/2})$	0.1159	0.1102		0.0627	0.0618
$C_3^0(s_{1/2})$	−0.0501	−0.0429		−0.0337	−0.0297

[a] H. Frank *et al.*, Phys. Lett. 19, 391, 719(E) (1965).
[b] Differs from the SP energy by a c.m. correction, Eqs. (II.15) and (II.18).
[c] Eigenseparation energy, BE(^{3}He) − BE(^{4}He) or BE(^{3}H) − BE(^{4}He).
[d] Centroid in $(p,2p)$ spectrum, H. Tyren *et al.*, Nucl. Phys. 79, 321 (1966).

mally occupied $0s_{1/2}$ shell, the energies of the normally empty states are lower (by ~2 MeV) for method IIC than for method I. They are also lower for valence "particles" than for the corresponding virtual states by ~2.5 MeV. The valence $0p_{3/2}$ SP energies in method IIC are, nevertheless, higher than the resonance energies obtained from nucleon scattering by about 4 MeV. 1 to 2 MeV of this difference is due, undoubtedly, to the truncation of the oscillator basis to three radial functions. This can be inferred from the variation of the SP energies with the number D of radial oscillator functions admixed. For example, for the neutron valence $0p_{3/2}$ state in method IIC, e(MeV) = 11.8 ($D=1$), 6.5 ($D=2$), and 9.3 ($D=3$). Moreover, close agreement between the RBHF valence energies and the resonance energies is not to be expected because the valence orbitals are not coupled to the "continuum."

The reason that a virtual state lies higher than the corresponding valence state is that the starting energy is less, which implies that the virtual excitations (in the ladders of interactions which are summed by the reaction matrix) occur with greater excitation energy. The matrix elements of t are therefore smaller in magnitude. Since the matrix elements are attractive they are less negative for off-shell than for on-shell interactions.

The wave functions of the $0p$ states tend to be closer to pure oscillator wave functions the lower their energies. Thus, the wave functions of method IIC are "purer" than those of method I, and those for valence states are less admixed than those of the corresponding virtual states. Recall from Table I that the $0s$ states had amplitudes of ~95% in the $0s$ oscillator state. Inaccuracies from truncation of the basis become more severe for higher-lying states and for properties which emphasize the surface as opposed to the nuclear interior.

The ^{4}He *point proton* or "body" densities, $\rho_B(r)$, obtained from the RBHF determinants in methods I and IIC, with r the distance from the center of the SP potential U (not from the c.m.), are displayed in Fig. 6 for the case of the Reid interaction. The volume integral of $\rho_B(r)$ is the charge $Z=2$. A striking effect of correcting the self-consistent field for c.m. motion is again clearly demonstrated: The curve for method IIC has a

TABLE II. RBHF calculations of the normally empty virtual $0p$ states in ^{4}He and the "valence" $0p$ states in ^{5}He and ^{5}Li performed with the Reid soft-core interaction, with $C=63.0$ MeV and $\alpha=0.65$ fm^{-1}. The dimensionality used was 4 for the s states and 3 for the p states. The results for c.m.-correction methods I and IIC are compared. For virtual "particles" $\bar{e}_p = 2\langle e_h\rangle - e_p$ [Eq. (II.b)] and for valence "particles" $\bar{e}_p = e_p$. Energies are in MeV. E_{res} and Γ are the resonance energy and width measured in nucleon scattering from ^{4}He.

	Virtual		Valence			
					Expt. [a]	
Method	I	IIC	I	IIC	E_{res}	Γ
			Neutrons			
$e_{0p_{1/2}}$	14.0	11.9	11.5	9.3	~3.6 ± 0.4	4 ± 1
$e_{0p_{3/2}}$	10.3	7.5	8.1	5.0	~1.0	0.6
$C_0^0(p_{1/2})$	0.7904	0.7787	0.8378	0.8422		
$C_1^0(p_{1/2})$	−0.5620	−0.5783	−0.5039	−0.5011		
$C_2^0(p_{1/2})$	0.2437	0.2433	0.2101	0.1989		
$C_0^0(p_{3/2})$	0.8353	0.8568	0.8722	0.9022		
$C_1^0(p_{3/2})$	−0.5071	−0.4802	−0.4521	−0.4023		
$C_2^0(p_{3/2})$	0.2125	0.1877	0.1867	0.1555		
			Protons			
$e_{0p_{1/2}}$	15.0	12.9	12.4	10.2	~9.5 ± 2.5	4 ± 1
$e_{0p_{3/2}}$	11.4	8.6	9.1	6.0	~2.0	1.5
$C_0^0(p_{1/2})$	0.7878	0.7750	0.8360	0.8397		
$C_1^0(p_{1/2})$	−0.5647	−0.5819	−0.5061	−0.5043		
$C_2^0(p_{1/2})$	0.2460	0.2466	0.2118	0.2013		
$C_0^0(p_{3/2})$	0.8325	0.8530	0.8704	0.8998		
$C_1^0(p_{3/2})$	−0.5106	−0.4857	−0.4549	−0.4067		
$C_2^0(p_{3/2})$	0.2150	0.1912	0.1885	0.1580		

[a] T. Lauritsen and F. Ajzenberg-Selove, Nucl. Phys. 78, 1 (1966).

much higher central maximum and then drops off more quickly for large values of r than does the curve for method I. The density shown in Fig. 6 is not to be directly compared with an "experimental" density inferred from elastic electron scattering.[57] A meaningful comparison requires (i) correcting the density of the independent particle model for the distribution of charge within the proton,[58] (ii) referring the theoretical density to the c.m. and (iii) including a modification of the theoretical single-proton density resulting from correlations between nucleons. Moreover, an empirical charge distribution cannot be uniquely determined from the measured absolute square of the form factor for elastic electron scattering $|F_{\rm chg}(q^2)|^2$. Even in the Born approximation, which is quite accurate for a nucleus with such a small charge as ^{4}He,[59] direct Fourier transformation from the measured $|F_{\rm chg}(q^2)|$ to the charge density relative to the c.m., $D_{\rm chg}(r')$ with $\vec{r}\,' = \vec{r} - \vec{R}$, is prevented by the limited range of momentum transfer for which the form factor is known, by the experimental errors for data in this range, and by the ambiguity in the sign of $F_{\rm chg}(q^2)$ for all but small values of q. Consequently, an "empirical" charge density is customarily obtained by assuming one or several analytical forms[60] for $D_{\rm chg}(r')$ and determining the parameters as those for which the calculated $|F_{\rm chg}(q^2)|$ is in best over-all agreement with the measured $|F_{\rm chg}(q^2)|$. In the Born approximation

$$F_{\rm chg}^{\rm Born}(q^2) = \frac{4\pi}{q}\int_0^\infty \sin(qr')D_{\rm chg}(r')r'dr' . \qquad \text{(III.3)}$$

A prejudice concerning the nature of $D_{\rm chg}(r')$ is contained in the choice of analytical forms considered. This fact has been emphasized by Friedrich and Lenz,[61] who have shown that the experimental data leave room for considerable uncertainty in the central density and in the presence or absence of oscillatory structure in $D_{\rm chg}(r')$.

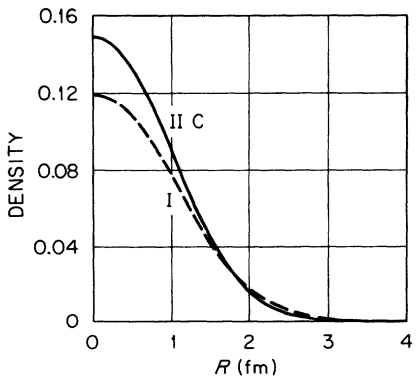

FIG. 6. Proton densities from RBHF calculations of ^{4}He using the Reid soft-core interaction (Ref. 39). The dimensionality is 4, $\alpha = 0.65$ fm^{-1}, and $C = 63.0$ MeV. The solid curve is for c.m. method IIC, the dashed curve for method I.

Over the range of momentum transfer for which electron-nucleus scattering has been carried out, the electric (or charge) form factor[62] of the proton $G_{Ep}(q^2)$ has been measured accurately and fitted rather closely by the "double pole" or "dipole" form factor[63]

$$G_{Ep}(q^2) \approx G_D(q^2) = (1 + 0.0556\,q^2)^{-2}, \qquad \text{(III.4)}$$

which corresponds to an exponential charge distribution in r. Here q is in inverse Fermis. In reducing electron scattering from a relativistic to a non-relativistic formalism,[64] there occurs a factor in $F_{\rm chg}(q^2)$, referred to as the Darwin-Foldy factor,

$$F_{\rm DF}(q^2) = 1 - 0.0042\,q^2, \qquad \text{(III.5)}$$

which is almost negligible for the existing experiments. Because G_{Ep} and $F_{\rm DF}$ are reliably known, it is convenient to compare experiment and theory through the values of a nonrelativistic-body form factor defined by

$$F_B(q^2) \equiv F_{\rm chg}(q^2)/\tilde{G}_{Ep}(q^2), \quad \tilde{G}_{Ep} = G_D F_{\rm DF} . \qquad \text{(III.6)}$$

In general F_B is complex, but for ^{4}He the imaginary part of F_B is expected to be significant only near the diffraction dip, $q^2 \approx 10$ fm^{-2}, where the Born approximation to F_B has a zero, and for values of q^2 larger than those measured so far ($q^2 \gtrsim 20$ fm^{-2}).

The structure of the proton is very important in analyzing the data. While it can be removed simply from the form factor, it cannot be unfolded easily from the charge density. Because of the smearing property of the convolution a great variety of body densities can lead to nearly the same charge distributions and, hence, nearly the same charge or body form factors over the measured range of q. Consequently, success in fitting the data by means of a certain $D_B(r)$ does not imply that the distribution of proton centers is actually that of D_B. Fitting $F_{\rm chg}$ is a necessary condition for the validity of D_B, but is by no means sufficient.

Rather extreme examples are provided by point-proton distributions with a hole in the center, such as the "double Gaussian"[65]

$$D_B^{\rm DG}(r') = N' e^{-\alpha^2 r'^2}(1 - e^{-\alpha^2 r'^2/\gamma^2}) . \qquad \text{(III.7)}$$

This density together with the corresponding charge density are shown in Fig. 12 of Ref. 65 for $\alpha^2 = 0.644$ fm^{-2} and $\gamma^2 = 0.190$. The point-proton distribution peaks at about 0.7 fm and decreases

rapidly for smaller r. The charge density on the other hand, looks very much like a normal distribution (single Gaussian) with a peak at the origin. The difference between D_B and $D_{\rm chg}$ in the example cited is an oscillatory function. But we know [see Eq. (III.6)] that $F_{\rm chg}(q^2)=F_B(q^2)\tilde{G}_{Ep}(q^2)$ in which $\tilde{G}_{Ep}(q^2)$ [Eqs. (III.4)–(III.6)] is smooth and monotonic. Thus, rather complicated differences between D_B and $D_{\rm chg}$ are transformed into simply and slowly varying differences between $F_B(q^2)$ and $F_{\rm chg}(q^2)$.

Successful fitting of $F_{\rm chg}$ by models with a hole in the center, such as the double Gaussian already cited,[65] or the densities obtained from a square-well SP potential with a hard core,[66] or a Morse potential[67] does not imply the existence of such a hole in the actual point-proton distribution. The repulsive core in the nucleon-nucleon interaction has led to speculation that such a hole might exist. For example, on p. 1186 of Ref. 65 the case of "four strongly attractive billiard balls" is cited. Classically, these "have a tetrahedron as their lowest-energy state and this has zero density in the middle." But one expects that quantum mechanically there is a great deal of zero-point motion. The self-consistent field approach leads one to believe that the zero-point motion almost entirely wipes out the classical tetrahedral structure. Even if the body density were to have a significant hole in the center, the dip in the charge density would not be pronounced. Tang and Herndon[68] have employed a trial wave function of the form

$$\psi=\prod_{i<j} f(r_{ij}), \tag{III.8}$$

which does not have dependence on the c.m., an advantage over the wave functions in self-consistent field theories. When f was calculated from a central exponential interaction with a hard core by means of the variational principle, the charge density did not have a dip at the origin, but rather a peak. Moreover, the peak was reduced only by ~13% when the hard-core radius was increased from 0.5 to 0.6 fm. (The core radius of the realistic Hamada-Johnston interaction[55] is 0.485 fm.) This is understandable if we recall that the rms charge radius of the proton is ≈0.8 fm, which is nearly twice the hard-core radius. Unfortunately, the body (proton) density was not given in Ref. 68.

Let us now turn to a major difficulty in all approaches which do not eliminate the c.m., in particular the self-consistent field approach. Given a nontranslationally invariant wave function such as the Slater determinant of the HF or RBHF theory, one must construct an "internal" (translationally invariant) wave function. This construction is not unique. For example, Lipkin[69] and Friar[70] have defined infinite families of internal wave functions Φ_μ obtainable from a given nontranslationally invariant one, Ψ. Here μ is a continuously variable parameter. Friar's transformation, which is closely related to Lipkin's, is expressed by

$$\Phi_\mu{}^2(\{\vec{r}_i'\})=N\int d^3R\, e^{-\mu R^2}\Psi^2(\{\vec{r}_i\}), \tag{III.9}$$

where

$$\vec{r}_i'=\vec{r}_i-\vec{R},\quad \vec{R}=A^{-1}\sum_{i=1}^{A}\vec{r}_i. \tag{III.9′}$$

The limiting cases $\mu=0$ and ∞ correspond to the well-known Gartenhaus-Schwartz (GS)[71] and fixed-c.m. (e.g., Refs. 65 and 72) transformations, respectively. Radhakant, Khadkikar, and Banerjee[72] have shown that the form factors $|F_{\rm chg}(q^2)|$ calculated from a certain shell-model density by means of the GS and fixed-c.m. transformations differ considerably from one another, both in the position of the diffraction minimum and the peak following the dip. The shell-model density was that of the s^4 configuration in which the radial function was a linear combination of $0s$ and $1s$ harmonic-oscillator functions ϕ_{ns}, i.e.,

$$R(r)=\frac{1}{(1+\beta^2)^{1/2}}[\phi_{0s}(r)+\beta\phi_{1s}(r)]. \tag{III.10}$$

Such a linear combination occurs in the $D=2$ (D = dimensionality) case of our work. Radhakant, Khadkikar, and Banerjee[72] simply varied β in order to produce a best fit to the form factor, finding a fair fit with $\beta=-0.32$ and the fixed-c.m. transformation; the GS curve for $\beta=-0.32$ gave a much worse fit. Ciofi degli Atti, Lantto, and Toropainen[73] produced, on the other hand, an excellent fit with this model [Eq. (III.10)] and the GS transformation when $\beta=-0.82$ [a huge admixture of ϕ_{1s}, giving a hole in the center of $\rho_B(r)$], whereas the fixed-c.m. transformation gave a very poor $|F_{\rm chg}(q^2)|$.

Other distributions with a hole in the center also give large differences between the form factors obtained with the GS and fixed-c.m. transformations. Friar[70] confirmed this strong sensitivity for the double-Gaussian density[65] [see Eq. (III.7)]

$$\Psi^2(\{\vec{r}_i\})=\prod_{i=1}^{4}\rho_B^{\rm DG}(\vec{r}_i) \tag{III.11}$$

and also showed that $|F_{\rm chg}|$ calculated with other values of μ, between 0 and ∞, lay between the GS and fixed-c.m. curves. Frosch's excellent fit[66] had been obtained with a SP potential consisting of a hard core followed by a deep narrow well, and with the GS transformation. Ciofi degli Atti, Lantto,

and Toropainen[73] found that the fixed-c.m. transformation applied to Frosch's shell-model density (which has a hole 1 fm in radius) gave an extremely poor fit.

At the opposite extreme is the nontranslationally invariant body density of the s^4 configuration of the harmonic-oscillator shell model, for which the corresponding translationally invariant density is the same for all values of μ because the wave function factors

$$\Psi^{\text{H.O.}}(r_1, \ldots, r_4) = \Phi_{0s}^{\text{H.O.}}(R)\Phi(r_1', \ldots, r_4') . \tag{III.12}$$

Tassie and Barker[74] showed that the form factor calculated with Φ is that calculated with $\Psi^{\text{H.O.}}$ divided by

$$\langle \Phi_{0s}^{\text{H.O.}}(R) | e^{i\vec{q}\cdot\vec{R}} | \Phi_{0s}^{\text{H.O.}} \rangle = e^{-b^2 q^2/4A}, \quad b = (\sqrt{2\alpha})^{-1} . \tag{III.13}$$

In our work the proton density (Fig. 5) can be fitted very closely by a harmonic-oscillator density. (The value of the inverse range parameter α is different from the value of α for the basis functions, ϕ_{nl}.) Thus, we have calculated F_B from the ρ_B obtained by employing the Tassie-Barker c.m. correction factor. This does lead to inaccuracies for large q values,[75] but in view of inaccuracies in the data, in the use of the first Born approximation, and in the truncation employed in performing the RBHF calculations it appears accurate enough for comparing the RBHF calculation with experiment. Campi, Martorell, and Sprung[76] have used the Tassie-Barker correction in their form-factor calculation based on a DDHF proton density.

Our body form factor for ^{4}He is shown in Figs. 7 and 8.[77] Figure 7 gives the traditional plot of $\ln|F_B(q^2)|$ for RBHF calculations with c.m. method IIC and dimensionality D (number of admixed harmonic-oscillator functions ϕ_{ns}) equal to 1 (curve labeled SOC), 2, 3, and 4. For $D=1$ and 3 there is no diffraction dip, but for $D=2$ and 4 there is a dip at $q^2 \approx 13$ fm^{-2}. The experimental dip occurs at about 10.5 fm^{-2}. It seems to us that the convergence of the form factor with increasing D is shown more clearly in the nonlogarithmic plot of $F_B(q^2)$ (Fig. 8). Only the absolute value of the experimental $F_B(q^2)$ is known, but from the theoretical values it seems reasonable to assume that $F_B^{\text{exp}}(q^2)$ is nearly real and positive for q^2 below 10 fm^{-2} and real and negative for $11 < q^2$

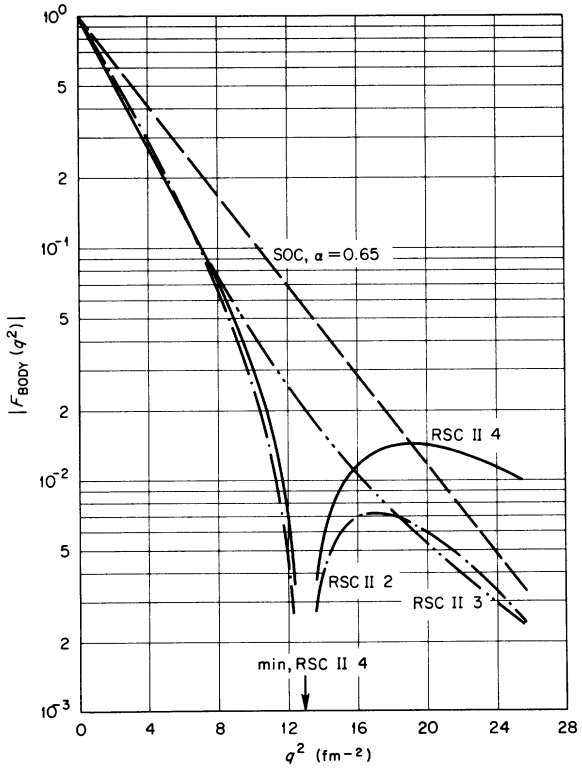

FIG. 7. A traditional semilogarithmic plot of $|F_{\text{body}}(q^2)|$ for ^{4}He vs q^2 for a dimensionality D of 1 (SOC), 2, 3, and 4. c.m. method IIC was employed.

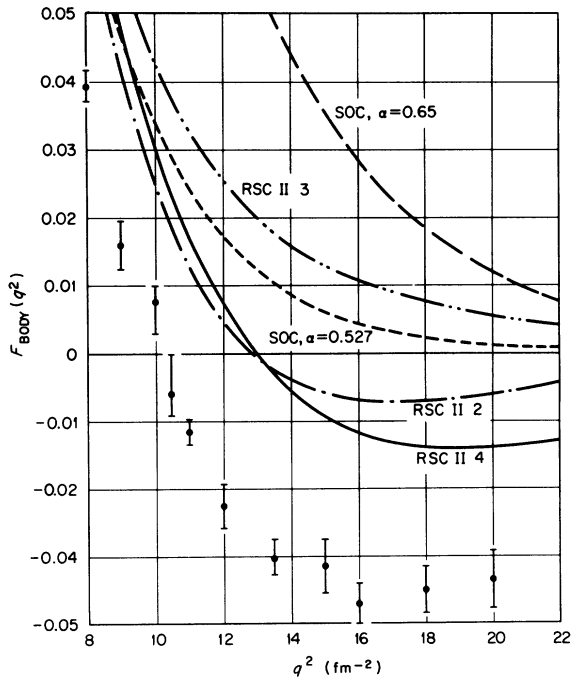

FIG. 8. A replotting of the curves of Fig. 7; $F_{\text{body}}(q^2)$ is given. "Experimental" values, calculated using Eq. (3.6) from the data of Ref. 57 are also shown. $F_{\text{body}}^{\text{exp}}$ is taken to be $\pm|F_{\text{body}}^{\text{exp}}|$ with the sign chosen in agreement with the RBHF value.

< 20 fm^{-2}. Near the diffraction dip F_B^{exp} cannot be assumed to be nearly real. It is clear from Figs. 7 and 8 that we have not used a large enough number of radial oscillator functions to have achieved convergence with D to the correct RBHF form factor. Before becoming greatly concerned with correlation corrections to the RBHF approximation, one should improve the accuracy with which the RBHF self-consistency conditions are satisfied by increasing D. Alternatively, one could evaluate the one-particle–one-hole correction terms for $\rho_B(r)$ in perturbation theory.[6] This has been done starting with a SOC ($D=1$) Slater determinant by Ciofi degli Atti and Kallio.[78] By increasing D in matrix-RBHF calculations we eliminate the contributions to these graphs from successively higher low-lying "particle" states. We believe it is more accurate to increase D than merely to calculate the 1p-1h graphs, because other aspects of self-consistency are also improved. In particular the SP energies change with the dimensionality. It was found in Ref. 78 that contributions from oscillator s states up to the $5s$ were important. Our $D_{max}=4$ calculation only included s states with $n \leq 3$.

Finally, we mention that for an accurate calculation of $F_B(q^2)$, contributions from correlation corrections to the RBHF determinant should be included. All the graphs through third order (second order in t and first order in the density operator) have been listed in Fig. 4 of Ref. 6. The low-q behavior of the form factor is

$$F_B(q^2) = 1 - \tfrac{1}{6}\langle r^2\rangle q^2 + 0(q^4) .$$

Kallio and Day[79] have calculated two of the correlation-correction diagrams for $\langle r^2\rangle$. These contain diagonal r^2 insertions in particle and hole lines, respectively, in the second-order 2p-2h excitation graph. It was found that the contribution from the insertion in the hole lines is roughly equal and opposite to that from the insertion in the particle lines, with the sum of the two contributions of the order of -0.09 fm^2. Later Ciofi degli Atti and Kallio[78] calculated the same graphs for the full form factor ($e^{i\vec{q}\cdot\vec{r}}$ insertions). The resulting contribution to $|F_B|$ is small ($\leq 10^{-2}$) and positive for all q. The 1p-1h corrections mentioned above are 10 times larger,[78] as can be seen also by comparing our results for $D=1$ and $D=4$.

We may summarize by saying that RBHF[3] or DDHF[76] calculations which give a good representation of the energetics of ^{4}He are also capable of giving a fairly good charge form factor. However, it should be emphasized that in the oscillator-basis matrix-RBHF approach, accurate calculations of the form factor and the excited states require a considerably higher dimensionality than do the binding energy and the hole-state energies. The primary reason for treating ^{4}He by the RBHF method is that, because so few doubly-closed-L-shell spherical nuclei exist in nature, namely ^{4}He, ^{16}O, and ^{40}Ca, it is important for the assessment of the method to calculate properties of ^{4}He. We have found that when c.m. corrections are included, the RBHF method describes ^{4}He rather well. However, for highest accuracy, other methods, which employ translationally invariant wave functions, should be preferred.

IV. RBHF CALCULATIONS FOR ^{16}O WITH THE HAMADA-JOHNSTON INTERACTION

In Tables III–V are presented results of RBHF calculations of properties of ^{16}O obtained with c.m.-correction methods I and IIC. By comparing with the corresponding quantities for ^{4}He, contained in Tables I and II, we see that there is much less difference in ^{16}O than in ^{4}He between the values given by methods I and IIC. For example, the calculated charge radius in ^{16}O is about 1.2% smaller with method IIC than for method I, whereas it was about 6% smaller for ^{4}He. This behavior is expected from the A^{-1} dependence of the c.m. corrections for the quantities considered. We may conclude that for nuclei heavier than oxygen, method I should be sufficiently adequate for binding and separation energies and true occupation probabilities.

Table III shows first of all that with the average off-energy-shell RBHF-self-consistent condition (Sec. II) for the well depth,[15,4,6] which led to $C=48.63$ MeV, the binding energy and removal energies are in generally good agreement with experiment. Notice that most of the SP energies are slightly more attractive for method IIC than for method I. The exceptions are the $0s_{1/2}$ neutron and proton energies, which can be explained as follows. The c.m. contribution tends to make the energies lower in method IIC than in method I. On the other hand, if the starting energies are lower in method IIC, then the reaction-matrix elements are less attractive and this tends to make the SP energies higher. These two effects are roughly equal in ^{16}O and, in the case of the most deeply bound states, the starting-energy effect dominates, thus giving SP energies which are slightly higher for method IIC than for method I. The difference in binding energies in Table III is due to self-consistency effects, just as in ^{4}He.

The binding per nucleon[3] for ^{16}O is very close to the experimental value[80] of 7.98 MeV. It is similar to those of SOC calculations with the same prescription for C[15,1,2,4,10] but it is significantly greater than the binding obtained in other BHF[30]

and RBHF[28,36,48] calculations. The greater binding occurs because the gap between occupied and unoccupied states is substantially smaller. However, the charge radius listed in Table III is somewhat further from the experimental value[81] of 2.666 ± 0.033 fm than the results obtained in Refs. 30, 28, 36, and 48. (It should be pointed out that the radius is less sensitive than the binding energy to the parameter C.[36]) This illustrates the general problem of correctly calculating both the binding energy and charge radius with presently available two-body interactions.[36,48]

The removal energies E^{I} in method I [Eq. (II.10)] differ by only a small c.m. correction from the SP energies e^{I}. In going beyond the nondegenerate perturbation theoretic formulation of Brueckner theory, employed in the present work, to a degenerate formulation[44] (e.g., the Bloch-Horowitz or the linked-valence expansion), the single-hole states can be mixed with two-hole–one-particle (and more complicated) states, resulting in a splitting of the single-hole strength.[82,6,83] The fractionation of single-hole strength becomes large when the hole is deep enough that there are two-hole–one-particle states which are quasi-degenerate with it.[82] This does not occur for the p shell in ^{16}O, but does occur for the s shell. The c.m.-corrected SP energy E_v then corresponds to

TABLE III. RBHF calculations for ^{16}O of the binding energy per nucleon; rms radii of the mass, neutron, and charge distributions; true occupation probabilities; Coulomb energies; and proton SP energies, removal-energy centroids, and eigenseparation energies. Neutron (ν) energies may be obtained by subtracting Δe_{Coul} from the proton (π) energies. The nucleon-nucleon interaction used is Hamada and Johnston's (Ref. 56), $\alpha = 0.45$ fm^{-1}, $C = 48.63$ MeV, and the dimensionality is 3 for all SP states.

c.m. method	I	Expt.	IIC
$-\mathcal{E}/A$ (binding per nucleon)	7.9	8.0	8.0
r_m (mass)	2.33		2.29
r_n (neutron)	2.33		2.29
r_c (charge)	2.47	2.666 ± 0.033 [a]	2.44
$P_{0p_{1/2}\nu} \approx P_{0p_{1/2}\pi}$	0.80		0.80
$P_{0p_{3/2}\nu} \approx P_{0p_{3/2}\pi}$	0.81		0.81
$P_{0s_{1/2}\nu} \approx P_{0s_{1/2}\pi}$	0.79		0.79
$\Delta e_{\mathrm{Coul}}(0p_{1/2})$	2.7	3.53 [b]	2.8
$\Delta e_{\mathrm{Coul}}(0p_{3/2})$	2.7	3.34 [b]	2.7
$\Delta e_{\mathrm{Coul}}(0s_{1/2})$	2.9		2.9
$e_{0p_{1/2}\pi}$	−15.0		−15.6
$E_{0p_{1/2}\pi}$	≈ -14.9	$-12.4^{+0.3}_{-1}$ [c]	≈ -14.9
$E^{(2)}_{\mathrm{rear}}(0p_{1/2})$	2.4 [d]		
$E^{(2)}_{e\,\mathrm{sep}}(0p_{1/2}\pi)$	−12.5	−12.13 [b]	
$e_{0p_{3/2}\pi}$	−18.5		−19.3
$E_{0p_{3/2}\pi}$	≈ -18.6	$-19.0^{+0.5}_{-1}$ [c]	≈ -18.6
$E^{(2)}_{\mathrm{rear}}(0p_{3/2})$	2.1 [d]		
$E^{(2)}_{e\,\mathrm{sep}}(0p_{3/2}\pi)$	−16.5	−18.46 [b]	
$e_{0s_{1/2}}$	−39.5(−46.5 [e])		−39.3(−46.3 [e])
$E_{0s_{1/2}}$	$\approx -38.5(-45.5$ [e])	-42 ± 5 [c]	$\approx -38.5(-45.5$ [e])
$E^{(2)}_{\mathrm{rear}}(0s_{1/2})$	13.7 [d]		
$E^{(2)}_{e\,\mathrm{sep}}(0s_{1/2}\pi)$	(31.8 [e])	−(28, 29.5, 32, 34) [c]	

[a] H. A. Bentz, Ref. 81.
[b] From energies of eigenstates in ^{15}N and ^{15}O.
[c] H. Tyren *et al.*, Ref. 85.
[d] SOC calculation by R. L. Becker and M. R. Patterson as quoted in Ref. 6.
[e] Includes a correction for c.m. spuriosity in the $(0s_{1/2})^{-1}$ hole state, Refs. 6 and 83.

the strength-weighted centroid of the energies of eigenstates of sharp l, j, and parity in the $A-1$ nucleus.[6,83] These centroids have been extracted, somewhat crudely so far, from $(p, 2p)$ and $(e, e'p)$ experiments and have been cited in Table III. For deep-lying holes an additional c.m. correction [over and above that of Eq. (II.8b)] is necessary in order to obtain the theoretical removal energy.[6,83] The need for this correction arises from the fact that a deep single-hole state of the oscillator shell model does not have the c.m. purely in its lowest oscillator state. The $(0s_{1/2})^{-1}$ state of the $A-1=15$ system is 20% spurious.[84] In a basis consisting of the $(0s_{1/2})^{-1}$ state together with all two-hole–one-particle states, degenerate with it (in the harmonic-oscillator shell model), two spurious states (states with the c.m. in an excited oscillator state) may be removed. This change of basis together with use of RBHF-SP energies caused the centroid of $0s_{1/2}$ strength in the shell-model calculation to be shifted downward by 7 MeV[6,83] to about −46 MeV for protons (see Table III).

The eigenstate of the $A-1$ nucleus with the greatest single-hole strength has an energy which differs from that of the centroid by a "rearrangement energy." The largest contribution in perturbation theory is expected to be the second-order energy $E^{(2)}_{\rm rear}(\mathrm{h})$ obtained from the diagram in Fig. 9(a).[82,27,6,83] In Fig. 9 the dashed hole lines are renormalized, i.e., multiplied by true occupation probabilities $P_{\rm h}$. The values of $E^{(2)}_{\rm rear}(nlj)$ calculated by Becker and Patterson[82,27,6] with the Hamada-Johnston interaction are quoted in Table III. One may then define an "eigenseparation energy"[6] (as opposed to a separation energy centroid)

$$E_{\rm esep}(nljq) = E(nljq) + E_{\rm rear}(nljq)\,. \qquad \text{(IV.1)}$$

The calculated eigenremoval energies are compared with the energies (relative to the ground state of ^{16}O) of specific eigenstates of ^{15}N in Table III. The rearrangement energy is j-dependent and increases the spin-orbit splitting of the $0p$ states by 0.3 MeV. The resulting theoretical splitting is only 4 MeV, however, which is about $\frac{2}{3}$ of the experimental value. For the highly excited $\frac{1}{2}^+$ states of ^{15}N, associated with a $0s_{1/2}$ hole, there are several peaks in the $(p, 2p)$ spectrum[85] which might correspond to the theoretical "dominant" eigenstate. The latter is rather uncertain because of the c.m. spuriosity effect, which should require a correction to Eq. (IV.1).

The SP energies of neutron states differ from those of the corresponding proton states by what is denoted by $\Delta e_{\rm Coul}(nlj)$ in Table III. In the RBHF theory this is actually not only a Coulomb energy, but contains a starting-energy self-consistency effect which tends to resist the Coulomb splitting. The shifts, $\Delta e_{\rm Coul}$, are smaller than the experimental differences between analogous states in ^{15}N and ^{15}O by a rather surprisingly large amount (~0.7 MeV) for the $0p_{3/2}$ and $0p_{1/2}$ states. Thus, only 80% of the experimental Coulomb splitting is found. The Coulomb interaction between protons is included as part of the two-nucleon interaction from which the SP potential is derived. It gives the largest contribution to the difference between neutron and proton orbitals. An additional contribution arises from the starting-energy self-con-

TABLE IV. Coefficients for the expansion of RBHF orbitals in terms of harmonic-oscillator orbitals. The interaction and parameters of the calculation are the same as those of Table III.

	Method I	Method IIC		Method I	Method IIC
Neutrons			Protons		
$C^0_0(s_{1/2})$	0.9997	0.9998	$C^0_0(s_{1/2})$	0.9998	0.9999
$C^0_1(s_{1/2})$	0.0241	0.0186	$C^0_1(s_{1/2})$	0.0172	0.0118
$C^0_2(s_{1/2})$	0.0089	0.0090	$C^0_2(s_{1/2})$	0.0086	0.0088
$C^0_0(p_{3/2})$	0.9995	0.9993	$C^0_0(p_{3/2})$	0.9993	0.9995
$C^0_1(p_{3/2})$	−0.0074	0.0239	$C^0_1(p_{3/2})$	−0.0166	0.0148
$C^0_2(p_{3/2})$	0.0315	0.0282	$C^0_2(p_{3/2})$	0.0326	0.0288
$C^0_0(p_{1/2})$	0.9979	0.9988	$C^0_0(p_{1/2})$	0.9974	0.9986
$C^0_1(p_{1/2})$	−0.0416	−0.0098	$C^0_1(p_{1/2})$	−0.0514	−0.0197
$C^0_2(p_{1/2})$	0.0494	0.0471	$C^0_2(p_{1/2})$	0.0512	0.0485

sistency. The expansion coefficients for the normally occupied neutron and proton orbitals are given in Table IV. The radii of neutron and proton distributions are the same to three significant figures.

Table V contains results for the normally empty (virtual) states of the s-d shell in ^{16}O and for the corresponding normally occupied (valence) states in ^{17}O and ^{17}F. The virtual states of the s-d shell have occupation probabilities of 1–2%, whereas those of the next higher f-p shell are 0.1–0.6% in a SOC calculation.[6] When the valence states are occupied their occupation probabilities were found to be comparable to (~5% greater than) those of the core orbitals.[27] The Coulomb energy differences between corresponding neutron and proton states are about $\frac{4}{5}$ of the experimental values.

The dimensionality of 3 seems to be sufficient for the reasonably accurate calculation of SP energies in the s-d shell. For example, the valence energies of the $0d_{5/2}$ ν and $0d_{3/2}$ π levels in method IIC are −0.71 and 7.23 with $D=1$ (SOC) and −0.98 and 5.90 with $D=3$, respectively. The c.m.-corrected separation ("addition") energies of these valence states are nearly the same for methods I and IIC, differing approximately [Eq. (II.18)] by only 0.04 MeV. The resulting addition energies for the s-d-shell orbitals are higher than the experimental eigenseparation energies by 3–4 MeV. This underbinding has occurred also in earlier SOC-RBHF calculations[4,10] which gave correctly the absolute binding energy of ^{16}O. The second- and third-order rearrangement energy diagrams for "particle" states shown in Figs. 9(b) and 9(c) have been investigated[6,27] to see if they would give additional binding. Values are quoted in Table V.

TABLE V. RBHF true occupation probabilities and energies of the s-d-shell orbitals in ^{16}O (virtual "particle" states) and in ^{17}O and ^{17}F (valence states). The SP energies of the virtual states were calculated from Eqs. (II.5) and (II.8b). Spin-orbit splittings are denoted by Δ_{so}; neutrons and protons are distinguished by ν and π. The interaction and the parameters used in the calculations are the same as in Table III.

		Virtual			Valence			
	Dimension:	SOC	$D=3$		SOC	$D=3$		
nlj	c.m. method:	I	I	IIC	I	I	IIC	$E_{esep}^{exp.}$
$0d_{5/2}$	$P(\nu)\approx P(\pi)$	0.012 [a]			0.865 [b]			
	Δe_{Coul}	3.57	2.99	3.02	2.87	2.75	2.79	3.54
	$e(\nu)$	7.28	4.71	4.50	−0.06	−0.55	−0.98	
	$e(\pi)$	10.85	7.70	7.52	2.81	2.20	1.81	
	$E(\nu)$					≈−0.25	≈−0.21	−4.14
	$E(\pi)$					≈ 2.54	≈ 2.58	−0.60
	$E_{rear}^{(2)}$	0.8 [a]			1.1 [a]			
	$E_{rear}^{(3)}$				−1.1 [b]			
$1s_{1/2}$	$P(\nu)\approx P(\pi)$	0.013 [a]			0.847 [b]			
	Δe_{Coul}		3.07	3.08		2.70	2.72	3.16
	$e(\nu)$	10.0 [a]	5.37	5.25	0.5	−0.40	−0.77	
	$e(\pi)$		8.44	8.33		2.30	1.95	
	$E(\nu)$					≈−0.04	≈ 0.00	−3.27
	$E(\pi)$					≈ 2.68	≈ 2.72	−0.11
	$E_{rear}^{(2)}$	1.0 [a]			1.4 [a]			
	$E_{rear}^{(3)}$				−1.0 [b]			
$0d_{3/2}$	$P(\nu)\approx P(\pi)$	0.021 [a]			0.859			
	Δe_{Coul}	3.54	2.70	2.70	2.86	2.62	2.63	3.56
	$e(\nu)$	14.21	8.40	8.33	5.01	3.41	3.27	
	$e(\pi)$	17.75	11.10	11.03	7.87	6.03	5.90	
	$E(\nu)$					≈ 3.99	≈ 4.03	≥0.94
	$E(\pi)$					≈ 6.62	≈ 6.66	≥4.50
	$E_{rear}^{(2)}$	1.5 [a]			1.9 [a]			
	$E_{rear}^{(3)}$				−0.9 [b]			
$0d_{3/2}$-	$\Delta_{so} E$					4.2	4.2	≥5.08
$0d_{5/2}$	$\Delta_{so} E_{rear}^{(2+3)}$				1			

[a] R. L. Becker and M. R. Patterson, as quoted in Ref. 6, to be described fully in Ref. 27. $C=47.753$ MeV was used.

[b] Reference 27.

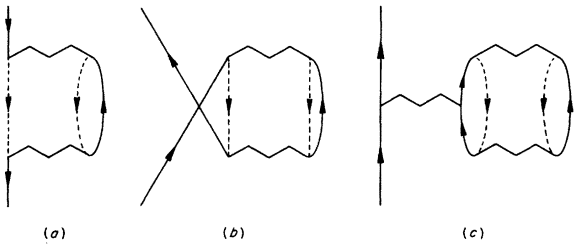

FIG. 9. Hole-line-renormalized rearrangement-energy diagrams (see Refs. 6 and 27). (a) $E^{(2)}_{\text{rear}}$ (h); (b) $E^{(2)}_{\text{rear}}$ (p); (c) $E^{(3)}_{\text{rear}}$ (p).

With SOC wave functions the results to date indicate near cancellation of the second- against the third-order rearrangement energy for the $0d_{5/2}$ state and a positive net contribution for the $1s_{1/2}$ and $0d_{3/2}$ states. For the $0d$ states this raises the calculated spin-orbit splitting from about 80 to 100% of the experimental value. However, another source of additional binding, such as orbital rearrangement energy, seems to be needed. More accurate (non-SOC) calculations of the rearrangement energies and of Pauli and spectral corrections to the reaction matrix elements would be desirable in this connection.

For ^{4}He we found a considerable difference between the RBHF proton densities given by c.m. methods I and IIC. For ^{16}O these densities are nearly identical and are unrecognizably different in appearance from that for the oscillator shell model (see, for example, p. 35 of Ref. 86). Some of the finer details of the RBHF densities are shown in Fig. 10. Both for methods I and IIC the $D=3$ RBHF densities are larger than the SOC density near the origin, smaller between 2 and 3 fm, and larger in the tail. The density $\rho^{\text{IIC}}(r)$ is slightly smaller than $\rho^{\text{I}}(r)$ near the origin, larger between $\frac{1}{2}$ and $2\frac{1}{2}$ fm, and smaller for $r \gtrsim 2\frac{1}{2}$ fm. Finally, in method IIC the neutron density is greater than the proton density for $r \lesssim 2\frac{1}{2}$ fm, and slightly smaller for larger r. The quality of the RBHF body form factor (not shown in a figure) as compared with the experimental data[87] is about the same as for ^{4}He. The considerable variation with dimensionality indicates, as in ^{4}He, the need for calculations with higher D. Thus, of the two main aspects of the "saturation properties" of finite nuclei (namely the energetics and the size) it appears that the energetics (binding energy and removal energies) and the rms radii are stable for a dimensionality of 3 or 4, but that the detailed shape of the density distribution requires a significantly more elaborate calculation.

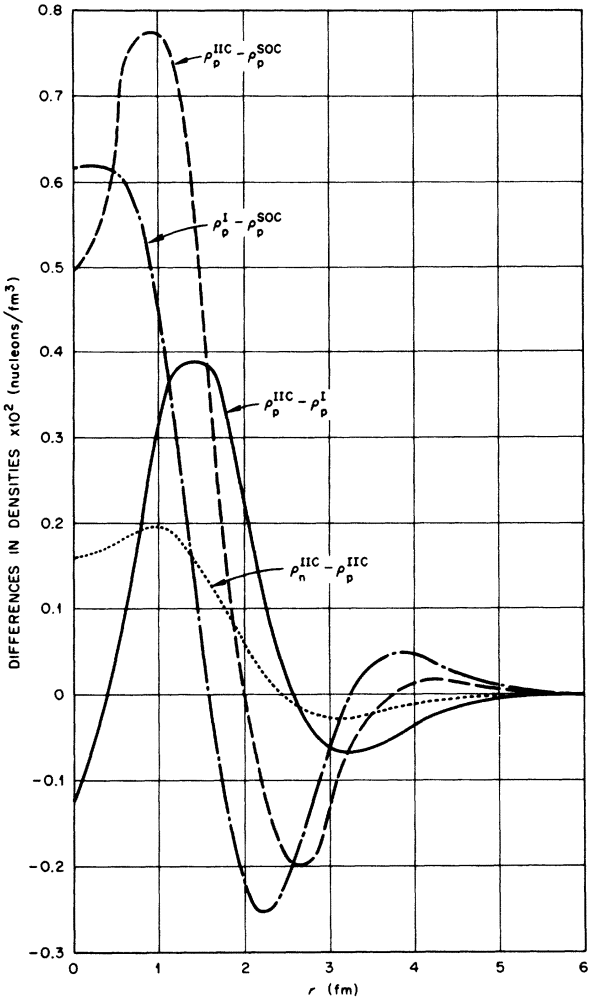

FIG. 10. Details of the RBHF density distributions for ^{16}O with a dimensionality of 3. Differences in densities, magnified by 100, are plotted. (a) Full curve, $\rho_p^{\text{IIC}}(r) - \rho_p^{\text{I}}(r)$; (b) dashed-dotted curve, $\rho_p^{\text{I}} - \rho_p^{\text{SOC}}$; (c) dashed curve, $\rho_p^{\text{IIC}}(r) - \rho_p^{\text{SOC}}(r)$; (d) dotted curve, $\rho_n^{\text{IIC}}(r) - \rho_p^{\text{IIC}}(r)$. The SOC density was calculated for $\alpha = 0.45$ fm^{-1}, the same value as for the basis orbitals of the $D=3$ calculation.

The main obstacle to such calculations is not the matrix diagonalization nor the self-consistency requirements, but the vastly greater number of two-nucleon reaction matrix elements which are needed. Their accurate calculation is very time consuming, requires a large amount of storage capacity, and would necessitate an order-of-magnitude increase in the RBHF computer technology.

The authors gratefully acknowledge discussions regarding this work with Michel Baranger, Baird Brandow, and Robert McCarthy.

*Research sponsored by U. S. Atomic Energy Commission under contract with Union Carbide Corporation.

[1]R. L. Becker and B. M. Morris, Bull. Am. Phys. Soc. 13, 1363 (1968).

[2]R. L. Becker and M. R. Patterson, Oak Ridge National Laboratory Physics Division Annual Progress Report for 1968, Report No. ORNL-4395 (unpublished), pp. 107–115.

[3]R. L. Becker and K. T. R. Davies, in *Proceedings of the International Conference on Properties of Nuclear States, Montréal, Canada, 1969*, edited by M. Harvey *et al.* (Univ. of Montreal Press, Montreal, 1969), p. 164; R. L. Becker, K. T. R. Davies, and M. R. Patterson, Oak Ridge National Laboratory Physics Division Annual Progress Report for 1970, Report No. ORNL-4659 (unpublished), pp. 26–28.

[4]R. L. Becker, Phys. Rev. Lett. 24, 400 (1970).

[5]R. L. Becker, Bull. Am. Phys. Soc. 17, 608 (1972); to be published.

[6]R. L. Becker, invited paper presented at the International Symposium on Present Status and Novel Developments in the Nuclear Many-Body Problem, Rome, 1972 (to be published).

[7]B. H. Brandow, Phys. Rev. 152, 863 (1966).

[8]K. A. Brueckner, Phys. Rev. 97, 1353 (1955); J. Goldstone, Proc. R. Soc. Lond. A293, 267 (1957). For a recent, lucid exposition of the elements of Brueckner theory, see B. D. Day, Rev. Mod. Phys. 39, 719 (1967); and for a review of its applications to infinite nuclear matter and finite nuclei, see H. A. Bethe, in *Annual Reviews of Nuclear Science*, edited by E. Segre *et al.* (Annual Reviews, Palo Alto, 1971), Vol. 21, p. 93.

[9]R. L. Becker, Phys. Lett. 32B, 263 (1970). The term "renormalized" Brueckner-Hartree-Fock theory (or approximation) was coined in this paper.

[10]R. L. Becker and M. R. Patterson, Nucl. Phys. A178, 88 (1971).

[11]T. Koopmans, Physica 1, 104 (1934).

[12]D. J. Thouless, (a) Phys. Rev. 112, 906 (1958); (b) *ibid.* 114, 1383 (1959).

[13]K. A. Brueckner and D. T. Goldman, Phys. Rev. 117, 207 (1960); L. M. Frantz and R. L. Mills, Nucl. Phys. 15, 16 (1960).

[14]H. A. Bethe, B. H. Brandow, and A. G. Petschek, Phys. Rev. 129, 225 (1963).

[15]R. L. Becker, A. D. MacKellar, and B. M. Morris, Phys. Rev. 173, 1264 (1968); in *Proceedings of the International Conference on Nuclear Physics, Gatlinburg, Tennessee, 12–17 September 1966*, edited by R. L. Becker, C. D. Goodman, P. H. Stelson, and A. Zucker (Academic, New York, 1967), p. 647.

[16]K. A. Brueckner, J. L. Gammel, and J. J. Kubis, Phys. Rev. 118, 1438 (1960).

[17]H. S. Köhler, Phys. Rev. 137, B1145 (1965).

[18]J. Dabrowski and H. S. Köhler, Phys. Rev. 136, B162 (1964).

[19]B. H. Brandow, Phys. Lett. 4, 8 (1963).

[20]C. W. Wong, Nucl. Phys. A104, 417 (1967).

[21]K. A. Brueckner, A. M. Lockett, and M. Rotenberg, Phys. Rev. 121, 255 (1961); K. S. Masterson, Jr., and A. M. Lockett, *ibid.* 129, 776 (1963); H. S. Köhler, Nucl. Phys. 38, 661 (1962); Phys. Rev. 138, B831 (1965).

[22]K. A. Brueckner and D. T. Goldman, Phys. Rev. 116, 424 (1959).

[23]H. S. Köhler and R. J. McCarthy, Nucl. Phys. A106, 313 (1967); R. J. McCarthy, *ibid.* A130, 305 (1969).

[24]B. H. Brandow, in *Lectures in Theoretical Physics*, edited by K. T. Mahanthappa and W. E. Brittin (Gordon and Breach, New York, 1969), Vol. XI-B, p. 55.

[25]B. H. Brandow, Ann. Phys. (N.Y.) 57, 214 (1970).

[26]See R. Rajaraman and H. A. Bethe, Rev. Mod. Phys. 39, 745 (1967).

[27]R. L. Becker and M. R. Patterson, to be published. Values of P_p's for spherical ^{12}C and for ^{16}O are quoted in Tables III and IV, respectively, of Ref. 6.

[28]R. J. McCarthy and K. T. R. Davies, Phys. Rev. C 1, 1644 (1970).

[29]R. L. Becker and R. W. Jones, Nucl. Phys. A174, 449 (1971).

[30]K. T. R. Davies, M. Baranger, R. M. Tarbutton, and T. T. S. Kuo, Phys. Rev. 177, 1519 (1969).

[31]K. T. R. Davies and R. L. Becker, Nucl. Phys. A176, 1 (1971).

[32]R. Muthukrishnan and M. Baranger, Phys. Lett. 18, 160 (1965); A. K. Kerman, J. P. Svenne, and F. M. H. Villars, Phys. Rev. 147, 710 (1966); K. T. R. Davies, S. J. Krieger, and M. Baranger, Nucl. Phys. 84, 545 (1966).

[33]R. M. Tarbutton and K. T. R. Davies, Nucl. Phys. A120, 1 (1968).

[34]M. K. Pal and A. P. Stamp, Phys. Rev. 158, 924 (1967); A. P. Stamp, Nucl. Phys. A105, 627 (1967); W. H. Bassichis, A. K. Kerman, and J. P. Svenne, Phys. Rev. 160, 746 (1967); S. J. Krieger, Phys. Rev. C 1, 76 (1970).

[35]K. T. R. Davies and M. Baranger, Phys. Rev. C 1, 1640 (1970).

[36]K. T. R. Davies and R. J. McCarthy, Phys. Rev. C 4, 81 (1971).

[37]R. C. Braley, W. F. Ford, R. L. Becker, and M. R. Patterson, Bull. Am. Phys. Soc. 16, 1165 (1971); W. F. Ford, R. C. Braley, R. L. Becker, and M. R. Patterson, *ibid.* 17, 506 (1972); R. L. Becker, R. C. Braley, W. F. Ford, and M. R. Patterson, Oak Ridge National Laboratory Report No. ORNL-TM-3951, 1972 (unpublished); W. F. Ford, R. C. Braley, R. L. Becker, and M. R. Patterson, invited paper presented at the Symposium on Present Status and Novel Developments in the Nuclear Many-Body Problem, Rome, Sept. 1972 (to be published).

[38]J. W. Negele, Phys. Rev. C 1, 1260 (1970).

[39]R. V. Reid, Ann. Phys. (N.Y.) 50, 411 (1968).

[40]P. Siemens, Nucl. Phys. A141, 225 (1970).

[41]K. A. Brueckner, J. L. Gammel, and H. Weitzner, Phys. Rev. 110, 431 (1958).

[42]J. Zofka and G. Ripka, Nucl. Phys. A168, 65 (1971).

[43]M. Baranger, in *Nuclear Structure and Nuclear Reactions, Proceedings of the International School of Physics, "Enrico Fermi," Course 40*, edited by M. Jean and R. A. Ricci (Academic, New York, 1969), p. 511.

[44]B. H. Brandow, Rev. Mod. Phys. 39, 771 (1967).

[45]K. A. Brueckner and J. L. Gammel, Phys. Rev. 109, 1023 (1958); S. Coon and J. Dabrowski, *ibid.* 140, B287 (1965).

[46]R. W. Jones and F. Mohling, Nucl. Phys. A151, 420 (1970).

[47]R. W. Jones, F. Mohling, and R. L. Becker, Nucl. Phys. (to be published).
[48]K. T. R. Davies, R. J. McCarthy, and P. U. Sauer, Phys. Rev. C 6, 1461 (1972).
[49]K. T. R. Davies, R. J. McCarthy, and P. U. Sauer, Phys. Rev. C 7, 943 (1973).
[50]A. D. MacKellar and R. L. Becker, Phys. Lett. 31B, 177 (1970).
[51]B. M. Morris and R. L. Becker, Bull. Am. Phys. Soc. 13, 628 (1968); and unpublished work.
[52]B. M. Morris, private communication.
[53]R. L. Becker and B. M. Morris, in *Proceedings of the International Conference on Nuclear Structure, Tokyo, Japan, 7–13 September 1967* (Univ. of Tokyo Press, Tokyo, 1967), p. 27.
[54]R. J. McCarthy, Nucl. Phys. A130, 305 (1969).
[55]See Ref. 4 for an application to ^{4}He with $m^*/m = 0.95$. More extensive SOC calculations employing m^* are contained in a paper in preparation by Becker, Morris, and Patterson.
[56]T. Hamada and I. D. Johnston, Nucl. Phys. 34, 383 (1962).
[57]R. F. Frosch, J. S. McCarthy, R. E. Rand, and M. R. Yearian, Phys. Rev. 160, 874 (1967).
[58]The contribution to elastic electron scattering from ^{4}He by the charge distribution within the neutrons is negligible for the existing experiments. Alternatively, since the neutron density is very nearly the same as the proton density, one may include the small contribution of the neutrons by employing the isoscalar charge density of the nucleon in place of the charge density of the proton. For a discussion of the influence of the electric form factor of the neutron on elastic electron scattering from nuclei, see W. Bertozzi, J. Friar, J. Heisenberg, and J. W. Negele, Phys. Lett. 41B, 408 (1972).
[59]R. Frosch, R. E. Rand, K. J. van Oostrum, and M. R. Yearian, Phys. Lett. 21, 598 (1966).
[60]R. Hofstadter and H. R. Collard, in *Landolt-Börnstein Numerical Data and Functional Relationships in Science and Technology*, edited by K. H. Hellwege and H. Schopper (Springer-Verlag, New York, 1967), New Series, Group I, Vol. 2, p. 21.
[61]J. Friedrich and F. Lenz, Nucl. Phys. A183, 523 (1972). See also H. A. Bethe and L. R. B. Elton, Phys. Rev. Lett. 20, 745 (1968).
[62]D. R. Yennie, M. M. Levy, and D. G. Ravenhall, Rev. Mod. Phys. 29, 144 (1957); F. J. Ernst, R. G. Sachs, and K. C. Wali, Phys. Rev. 119, 1105 (1960); R. G. Sachs, *ibid.* 126, 2256 (1962); L. N. Hand, D. G. Miller, and R. Wilson, Rev. Mod. Phys. 35, 335 (1963).
[63]L. H. Chan, K. W. Chen, J. R. Dunning, N. F. Ramsey, J. K. Walker, and R. Wilson, Phys. Rev. 141, 1298 (1966); M. Goitein, J. R. Dunning, and R. Wilson, Phys. Rev. Lett. 18, 1018 (1967).
[64]K. W. McVoy and L. van Hove, Phys. Rev. 125, 1034 (1962).
[65]R. H. Bassel and C. Wilkin, Phys. Rev. 174, 1179 (1968).
[66]R. Frosch, Phys. Lett. 37B, 140 (1971). See also B. F. Gibson, A. Goldberg, and M. S. Weiss, Nucl. Phys. A111, 321 (1968).
[67]A. Gersten and A. E. S. Green, Bull. Am. Phys. Soc. 13, 627 (1968).
[68]Y. C. Tang and R. C. Herndon, Phys. Lett. 25B, 307 (1967).
[69]H. J. Lipkin, Phys. Rev. 110, 1395 (1958).
[70]J. L. Friar, Nucl. Phys. A173, 257 (1971).
[71]S. Gartenhaus and C. Schwartz, Phys. Rev. 108, 482 (1957).
[72]S. Radhakant, S. B. Khadkikar, and B. Banerjee, Nucl. Phys. A142, 81 (1970).
[73]C. Ciofi degli Atti, L. Lantto, and P. Toropainen, Phys. Lett. 42B, 27 (1972).
[74]L. J. Tassie and F. C. Barker, Phys. Rev. 111, 940 (1968).
[75]F. A. Gareev and F. Palumbo, Phys. Lett. 40B, 621 (1972).
[76]X. Campi, J. Martorell, and D. W. L. Sprung, Phys. Lett. 41B, 443 (1972).
[77]These figures have been presented earlier in the talk cited in Ref. 6.
[78]C. Ciofi degli Atti and A. Kallio, Phys. Lett. 36B, 433 (1971).
[79]A. Kallio and B. D. Day, Nucl. Phys. A124, 177 (1969).
[80]A. H. Wapstra, Physica 21, 367 (1955).
[81]H. A. Bentz, Z. Phys. 243, 138 (1971).
[82]R. L. Becker and M. R. Patterson, Bull. Am. Phys. Soc. 15, 1315 (1970). The results for $E^{(2)}_{\text{rear}}$, Figs. 9(a) and 9(b), are listed in Table I of Ref. 6.
[83]R. L. Becker, Oak Ridge National Laboratory Physics Division Annual Report for 1972, Report No. ORNL-4844, 1973 (unpublished), p. 10; Bull. Am. Phys. Soc. 18, 576 (1973); to be published.
[84]The only reference we have found which contains this little known but important fact is Edith Halbert's Ph.D. thesis, University of Rochester, 1956 (unpublished).
[85]H. Tyren, S. Kullander, O. Sundberg, R. Ramachandran, and P. Isacsson, Nucl. Phys. 79, 321 (1966).
[86]L. R. B. Elton, *Nuclear Sizes* (Oxford U. P., London, 1961).
[87]I. Sick and J. S. McCarthy, Nucl. Phys. A150, 631 (1970); and I. Sick, private communication.